New Techniques to Efficiently Determine Proximity to Static Voltage Collapse

by

Antonio Carlos Zambroni de Souza

A thesis
presented to the University of Waterloo
in fulfilment of the
thesis requirement for the degree of
Doctor of Philosophy
in
Electrical Engineering

Waterloo, Ontario, Canada, 1996

I hereby declare that I am the sole author of this thesis.

I authorize the University of Waterloo to lend this thesis to other institutions or individuals for the purpose of scholarly research.

I further authorize the University of Waterloo to reproduce this thesis by photocopying or by other means, in total or in part, at the request of other institutions or individuals for the purpose of scholarly research.

The University of Waterloo requires the signatures of all persons using or photocopying this thesis. Please sign below, and give address and date.

Abstract

This thesis studies the voltage collapse phenomena in power systems. Bifurcation theory is briefly discussed, and it is shown that a saddle-node bifurcation is the generic bifurcation identified by the power-flow equations used here. A continuation program is used to trace the bifurcation manifold and determine the saddle-node bifurcation point.

A voltage collapse index by reduced Jacobian determinant is proposed and compared to other previously proposed indices. This thesis describes all these indices and points out the particular characteristics of each one. Critical bus determination is also discussed.

Network partitioning, initially proposed for a general netlist, is extended to power systems by means of different techniques. These methodologies are compared, and their computational features are discussed as well. Advantages and disavantages of each partitioning and reduction technique are studied, and a particular method is recommended based on its computational requirements.

Acknowledgements

I would like to thank CNPq, a brazilian agency of education, for their indispensable sponsorship in this work.

I wish to thank my supervisors Victor H. Quintana and Claudio Cañizares, for their guidance and friendship. I also thank them for the skills they have taught me and the confidence shown in my abilities.

I gratefully thank my wife Marli, for her love and support ever since we met. With her, my dreams became true. I thank my parents, for all the sacrifice they have done toward my education. They gave me the love that has been the compass of my life.

Dedication

This thesis is dedicated to my beloved son, Matheus.

Contents

List of Tables

List of Figures

Chapter 1

A BRIEF HISTORICAL REVIEW

1.1 Introduction

Voltage stability problems have received increased attention over the last few years. Many published papers have demonstrated the importance of the problem and several occurrences all around the world have shown that the problem may have serious consequences [1, 2, 3], such as excessive voltage drop or dynamic instability. Since power systems are operated under increasingly stressed conditions, the ability to maintain voltage stability has become a growing concern, and good measures to improve the reactive power and voltage level control are required. If effective control actions are not appropriately implemented, successive load increases may drive a system to an unstable state, at which abnormal operating conditions can be identified. The following formal definitions of terms related to voltage collapse are given in reference [4] :

- Voltage Stability is the ability of a power system to maintain voltage so that when load admittance is increased, load power will increase, and so both power and voltage are controllable.
- Voltage Collapse is the process by which voltage instability leads to loss of voltage in a significant part of a power system.
- Voltage Security is the ability of a power system, not only to operate stable but also to remain stable following any reasonably contingency or adverse system change.

A system becomes unstable when a disturbance (load increase or other system change) causes voltage to drop quickly or drift downward, and operators and automatic system controls fail to improve the voltage level. The voltage decay may take from a few seconds to several minutes.

The following list provides some voltage collapse events all around the world [4]:

- Incident in South Zealand, Denmark, March 1979.
- Incident in the southern part of the Nordel system (Sweden and Denmark), December 1983.
- Incident in Czechoslovakia, July 1985.
- Incident in England, May 1986.

Reference [4] shows that each one of these events occurred due to different reasons. Hence, many discussions on the nature of voltage collapse have taken place, e.g., references [3, 5, 6] have associated voltage collapse to a bifurcation point, and this approach is employed in this thesis. However, several kinds of bifurcation are found

in the literature, and each one has different characteristics [7]. References [8, 9] have shown that voltage collapse can be associated in some cases to a Saddle-Node bifurcation. This chapter presents some of the issues about the nature of voltage collapse that have been discussed in recent publications.

1.2 Voltage Collapse Phenomenon

The list of events described in the foregoing section shows that voltage collapse is a real problem, and its consequences may be dramatic. An analysis of each of those events may help one understand how voltage collapse can be identified and prevented in a power system. The incidents in Denmark and England were characterized as slow events, whereas the incidents in Sweden and Czechoslovakia were fast events. Therefore, it is necessary to establish which kind of event would be analyzed in order to define an approach to study the problem.

For example, a fast voltage collapse may be triggered by the loss of a transmission line or a generator. If the dynamic response of the system is not strong enough to overcome the fault, the system looses stability. The analysis of this phenomenon requires a detailed system model, including the transient equations of generators. On the other hand, a power system may be driven to voltage collapse by small signal perturbations. In this situation a system may collapse because some transmission lines reach the maximum power that can be transmitted or because of lack of local reactive power support. This kind of voltage collapse is defined as a static voltage problem. A detailed system model identifies this phenomenon. Some researchers, however, have shown that under certain conditions, the power flow equations may be used to study this kind of voltage collapse problem. This system model is used in this thesis, limiting the scope of this work to static voltage collapse.

1.3 Dynamic vs. Static Analysis

Voltage collapse has most frequently been studied via power flow simulations. Long-term voltage collapse can be approximated by power flow "snapshots" at tens of seconds or minutes following major outages. In steady-state cases, most of the voltage collapse indicators are based on load-flow feasibility [10] or steady-state stability [11]. Examples of this approach can be found in references [12, 13] where voltage collapse is explained as a static bifurcation phenomenon. Although these references have provided tools to analyze the voltage stability of an operating point, measures to alleviate a power system that is working close to voltage collapse are not discussed. This handicap is overcome in reference [14], where controllability concepts are applied to solve the voltage stability problem. In reference [14] it is assumed that no active power variations occur in a power system, only reactive power variations are considered with the swing bus absorbing all active variations, which is not a good model since in a real power system all the generators share the active power variation. These considerations allow one to reduce the Jacobian (including the reactive power equations associated to PV buses) only to the partial derivatives of the reactive power equations in relation to voltage level variation. Manipulations of the reduced Jacobian provide the sensitivity matrices that identify the weak area of a power system and the proper control actions associated to that specific operating point.

References [15, 16, 17] show that under certain conditions, voltage collapse analysis by static and dynamic approaches lead to similar results, with static analysis being sometimes preferred due to smaller computational time requirements. Reference [16], however, points out that dynamic characteristics of synchronous machines must be considered.

Evaluation of eigenvalues has been employed in voltage collapse analysis [18, 19] as an extension to small signal perturbation analysis of power system [20, 21]. However, evaluation of eigenvalues is required for each operating point, which may be time consuming.

Notice, however, that small signal perturbation analysis can not be applied to dynamic voltage stability studies. The problem of dynamic voltage stability is not in the same spectrum as the static voltage stability problem analyzed here because of the time frame involved in each one; static voltage stability requires minutes to hours of analysis, and dynamic voltage stability requires miliseconds to seconds.

1.4 Energy Function Technique

Energy functions were initially employed in power systems to study transient stability analysis. The method consists of evaluating the total energy (kinetic and potential) of a power system during a faulted operation. In order for the system to remain stable, this energy has to match a certain energy level associated with the post-fault condition; this methodology determines the critical clearing time for which a system is stable. References [22, 23] have employed this technique in order to evaluate the critical clearing time associated with a fault. The method may provide wrong results since damping and more complex models are not considered.

The method, however, has been successfully employed in references [24, 25, 26, 27] to evaluate voltage collapse conditions. This can be done because for static voltage collapse analysis only the potential energy of the system is considered, which does not require damping inclusion or complex generator models. References [24, 26] show that an energy function variation has a linear behavior in relation to a load increase, which provides a relative measure of the energy index for any

operating point. Since the system loading distance to the bifurcation point may be evaluated from an energy function, information about load margin may be obtained for any operating point, which is another important aspect to be considered.

This work does not employ energy functions as a voltage collapse tool, rather, new techniques that are not dependent on system models are proposed. These techniques identify saddle-node bifurcation for any non linear system.

1.5 Load Margin and Bifurcation Point Determination

By load margin one means the load variation necessary to take a system to the voltage collapse point. Reference [28] has employed load margin as a control action, when it is used to calculate load shedding to maintain a system in a safe region of operation. In most cases, however, the load margin is calculated to evaluate the voltage security level of a system. Reference [29] presented a method that reduces the load-flow Jacobian to the reactive power equations, as done in reference [14], and calculates the load margin through non-linear optimization, resulting in similar equations as in [6]. After calculating the load margin, the power factor is assumed constant and the active load variation is determined. However, [6, 12] show that the voltage collapse point determination is better done by the use of active and reactive power equations.

An effective method to evaluate load margin of a power system is the continuation method [25]. Such a method overcomes the singularity of the load-flow Jacobian at the voltage collapse point. This feature allows one to trace the curve of voltage level variation as a function of load variation, also known as voltage profiles.

Since this method may consider any system model, an accurate answer is obtained. On the other hand, the method is time consuming due to the dimension of the systems involved. This handicap is overcome if a network partitioning technique is applied, since the load margin may be easily evaluated if the weak area of a power system is identified (the weak area is a small part of a power system).

1.6 Network Partitioning Technique

It has been shown that voltage collapse starts locally and spreads to the neighboring buses. Therefore, for a known operating point, it is possible to evaluate the security level of a whole system through evaluation of a small part of the system. Reference [24] has shown that a power system may be partitioned using the Ward method, which consists of retaining the buses of interest through manipulations of the Y matrix. However, in this reference the critical bus of a system is not identified, which requires several partitions in order to evaluate the voltage security.

Determination of critical areas has been proposed in references [30, 31], where eigenvalues and singular values decomposition are employed. The identification of these areas allows one to determine the control actions for a known operating point. References [32, 33, 34] proposed a network partitioning based on a reduced load-flow Jacobian determinant. The Jacobian is reduced to a 2x2 matrix according to the bus of interest. The smallest determinant provides the critical bus for that operating point. References [35, 36], however, show that the critical bus of an initial operating point may not be same at the bifurcation point, and this possibility should not be neglected, especially‘ for a large system.

Network partitioning has not been exhaustively studied in voltage collapse analysis. Reference [37] determines the critical area of a power system through eigen-

values technique. Reference [38] evaluates the buses, branches and generators participation on voltage collapse, identifying the critical areas of a system, using eigenvalue techniques. Reference [39] presents a bus cluster based on sensitivity matrices and reference [40] proposes a clustering algorithm based on graph theory. These techniques provide good results.

1.7 Organization

The aim of this work is to propose a technique that can be used to evaluate the proximity to voltage collapse of a power system. The work is organized as follows. Chapter 2 presents a brief discussion on system modelling and bifurcation theory. Chapter 3 discusses bifurcation in power systems, reduced load-flow Jacobian determinant, modal analysis and test functions. Chapter 4 discusses continuation and direct methods, and network partitioning techniques. Chapter 5 shows the results of these techniques on a 300 bus test system, and compares the results. The tests are divided as follows:

1. Voltage collapse analysis through reduced Jacobian determinant [33, 32, 34]. This technique is compared with eigenvalues and singular values decomposition and test function techniques, and good results are obtained. A new contribution is the proposal of this methodology as a voltage collapse index. The comparison of reduced Jacobian determinant to eigenvalues and singular values decomposition and test functions provides an insight into those techniques, which has not been addressed by the original authors; this is another contribution of this thesis.

2. Network partitioning implementation to reduce the computational burden. New techniques based on reduced Jacobian determinant, right-eigenvector and tangent vector are proposed. These methodologies are then mixed with a system reduction technique proposed in [36], with good results.

Finally, Appendix A briefly describes the PFLOW program used in Chapter 5.

Chapter 2

STABILITY CONCEPTS AND SYSTEM MODELING

2.1 Introduction

This chapter describes some basic principles of stability for further application in power systems. The system model used throughout this thesis is also presented.

2.2 Definitions of Stability

Physical systems are described by their mathematical models for purposes of analysis. A description of the dynamics of some systems is given by one of the following differential equations:

1. $\dot{x} = f(x, u, t) \rightarrow$ Nonlinear, time varying and forced system
2. $\dot{x} = f(x, t) \rightarrow$ Nonlinear, time varying and force free system

3. $\dot{x} = f(x, u) \rightarrow$ Nonlinear, time invariant and forced system

4. $\dot{x} = f(x) \rightarrow$ Nonlinear, time invariant and force free system

where x represents the state variables, u represents the input control variables and t is the independent time variable. The system represented by equation (4) is called an autonomous system, and is typically used to describe power systems.

The direct method of Lyapunov is an efficient approach to the problem of stability [41]. The method is based on the following reasoning. If the rate dE/dt of the energy $E(x)$ of an isolated physical system is negative for every possible state x except for a single stable equilibrium state x_e, then the energy will decrease continually until it finally assumes its minimum value E(x_e) . If for that system one is able to find a function $V(x)$ such that it is always positive except at $x = x_e$, at which point it is zero, and its derivative $dV/dt < 0$ except at $x = x_e$, where it is zero, then the system returns to x_e if it is disturbed. The function $V(x)$ is called a Lyapunov function.

Lyapunov functions were initially used in power systems for transient stability analysis [22, 23]. In that context, a large disturbance is first applied to the system, which gives the system some initial energy. Following the disturbance, a time invariant system model is assumed, so that the existence of a time invariant energy follows. If the initial energy following the disturbance is less than that of the post-fault system's unstable equilibrium point (u.e.p.) with the lowest energy, the system will return to its post-fault equilibrium point. The method can be explained using the analogy of the ball in the well shown in Figure 2.1.

The well has an asymptotically stable equilibrium point (s.e.p.) x_e at the local minimum of the potential energy function, and a (u.e.p.) x_u at the local maximum. Assume that the ball is initially at x_e, and it is displaced from the s.e.p. by

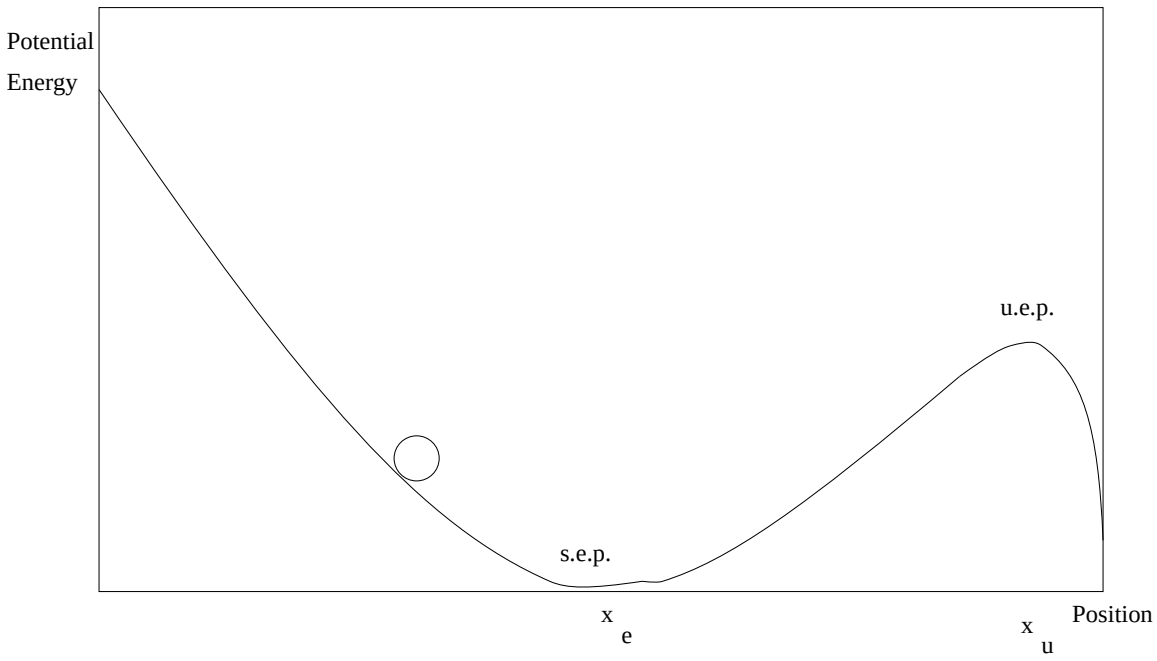

Figure 2.1: A ball in the well example.

some type of disturbance. The problem then is to determine whether, following a disturbance, the ball would eventually return to the (s.e.p.). In this example, the maximum point that the ball could reach would be the point associated to the same energy level as x_u. However, an initial point with an energy level greater than x_u cannot be defined unstable a priori, since the system damping has to be considered.

For static voltage collapse analysis, a system is not subjected to a large disturbance. Rather the operating point of the system is moving in a "quasi-static" manner. Hence, even though the dynamic characteristics are considered, a steady-state analysis may be carried out.

The two-bus lossless system shown in Figure 2.2 is used here to illustrate the static voltage collapse problem. First, assume that the real power demand at Bus 2 is a constant plus a linear term dependent on bus frequency. This follows the

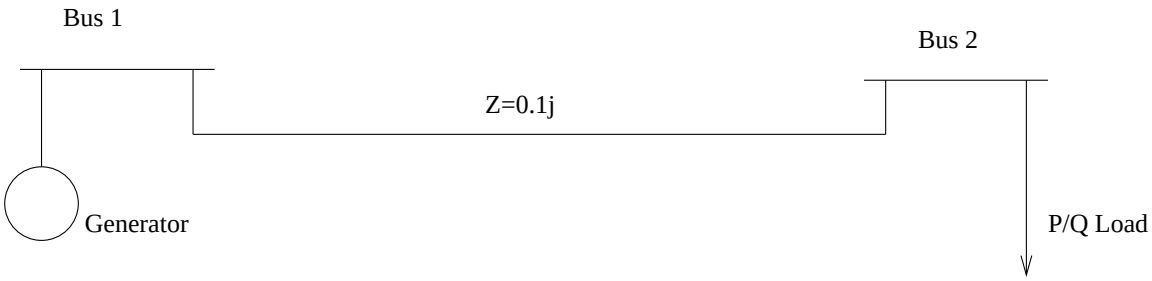

Figure 2.2: A two-bus lossless system.

structural preserving model for transient stability analysis discussed in [42]. Using the classical model for the generator and dynamic load model, the system equations are then given by

$$M_g\,\dot{\omega} \;+\; D_g\,\omega \;-\; B_{12}\,V\,\sin(\delta_1 \;-\; \delta_2) \;+\; P_L = 0 \tag{2.1}$$

$$-(P_L \;+\; D_L\,\dot{\delta}_2) \;=\; B_{12}\,V\,\sin(\delta_2 \;-\; \delta_1) \tag{2.2}$$

$$-Q_L \;=\; T\,V\,\dot{V} \;-\; B_{22}\,V^2 \;-\; B_{21}\,V\,\cos(\delta_2 \;-\; \delta_1) \tag{2.3}$$

Under the assumptions that $P_M = P_L$ (generator mechanical power matches active load demand) and $B_{12} = B_{21}$, these equations may be written as

$$\dot{\omega} \;=\; -M_g^{-1}\,D_g\,\omega \;+\; M_g^{-1}\,f(\alpha, V) \tag{2.4}$$

$$\dot{\alpha} \;=\; -D_L^{-1}\,f(\alpha, V) \;-\; \omega \tag{2.5}$$

$$T\,\dot{V} \;=\; -V^{-1}\,g(\alpha, V) \tag{2.6}$$

where

- $M_g \rightarrow$ Inertia constant of the generator
- $D_L, \quad D_g \rightarrow$ Damping of load and generator
- $f(\alpha, V) = P_L + B_{12}\ V\ sin(\alpha)$
- $g(\alpha, V) = Q_L$ - $B_{12}\ V\ cos(\alpha)$ - $B_{22}\ V^2$
- $\omega = \dot{\delta}_1$
- $V \rightarrow$ Voltage magnitude at Bus 2.
- P_L and $Q_L \rightarrow$ Active and reactive load at Bus 2.
- $\alpha \rightarrow$ Angular difference between Buses 2 and 1, i.e., $\delta_2 - \delta_1$
- $B_{12} = B_{21} \rightarrow$ Susceptance between Buses 1 and 2.
- T $\rightarrow$ Voltage time constant.

Hence, in this case

$$\begin{bmatrix} \dot{w} \\ \dot{\alpha} \\ \dot{V} \end{bmatrix} = \begin{bmatrix} -M_g^{-1} D_g M_g^{-1} & -M_g^{-1} & 0 \\ M_g^{-1} & -D_L^{-1} & 0 \\ 0 & 0 & 1/T \end{bmatrix} \begin{bmatrix} M_g w \\ f(\alpha, V) \\ V^{-1} g(\alpha, V) \end{bmatrix} \tag{2.7}$$

Defining A as the 3x3 matrix above, $x = [w \quad \alpha \quad V]^T$, and $\phi(x) = [M_g w \quad f(\alpha\,, V) \quad V^{-1}\, g(\alpha\,, V)]^T$, a Lyapunov function can be defined as [24, 25]:

$$V(x, x_e) \quad = \quad \int_{x_e}^{x} [\phi(x)]^T \ dx \tag{2.8}$$

where V(x) is locally positive definite about x_e, and

$$\dot{V}(x) \;=\; \nabla^T V(x)\;\dot{x} \;=\; \frac{1}{2}\;\nabla^T V(x)\;\;(A + A^T)\;\;\nabla V(x) \;\leq\; 0 \qquad (2.9)$$

Therefore, for a lossless two-bus system, a Lyapunov function (V(x)) has been established. The graphic of Figure 2.3 shows the most important characteristic of the energy function for steady-state voltage collapse analysis, which is its quasi-linear behavior in relation to a load increase. The power factor is kept constant during this load increase. Figure 2.4 shows the PV curve, i.e., the plot of V with respect to P_L , where V and P_L are the voltage level and active power demand at bus 2, respectively. Figure 2.3 was obtained for the power system shown in Figure 2.2, and so is Figure 2.4, with $B_{12} = 10$ and $B_{22} = -10$.

Since equation (2.8) can be shown to correspond to an area between the u.e.p. and s.e.p. [24, 26]. For example, in Figure 2.4, for $P_L = 1.0$, the energy at that point is the area of the PV curve defined by the P_L interval [1.0, 3.0]. The point $P_L = 3.0$ is the maximum load that can be transmitted between buses 1 and 2, and is also the system saddle-node bifurcation point.

Figure 2.3 helps one understand the voltage collapse process. For the initial operating point, the associated energy $V(x)$ represents a region of stability. As the system is loaded, the energy level is reduced and so is the region of stability. When the system reaches the bifurcation point the region of stability vanishes, and the system becomes unstable. For the bifurcation point ($P_L = 3$ in Figure 2.4), a zero real eigenvalue of the dynamic Jacobian of equations (2.7) is encountered; this feature has been largely exploited in the literature [18, 34, 38, 43].

The phenomenon of loss of stability at the bifurcation point may be shown through time domain simulation of equations (2.4) to (2.6). The load is kept con-

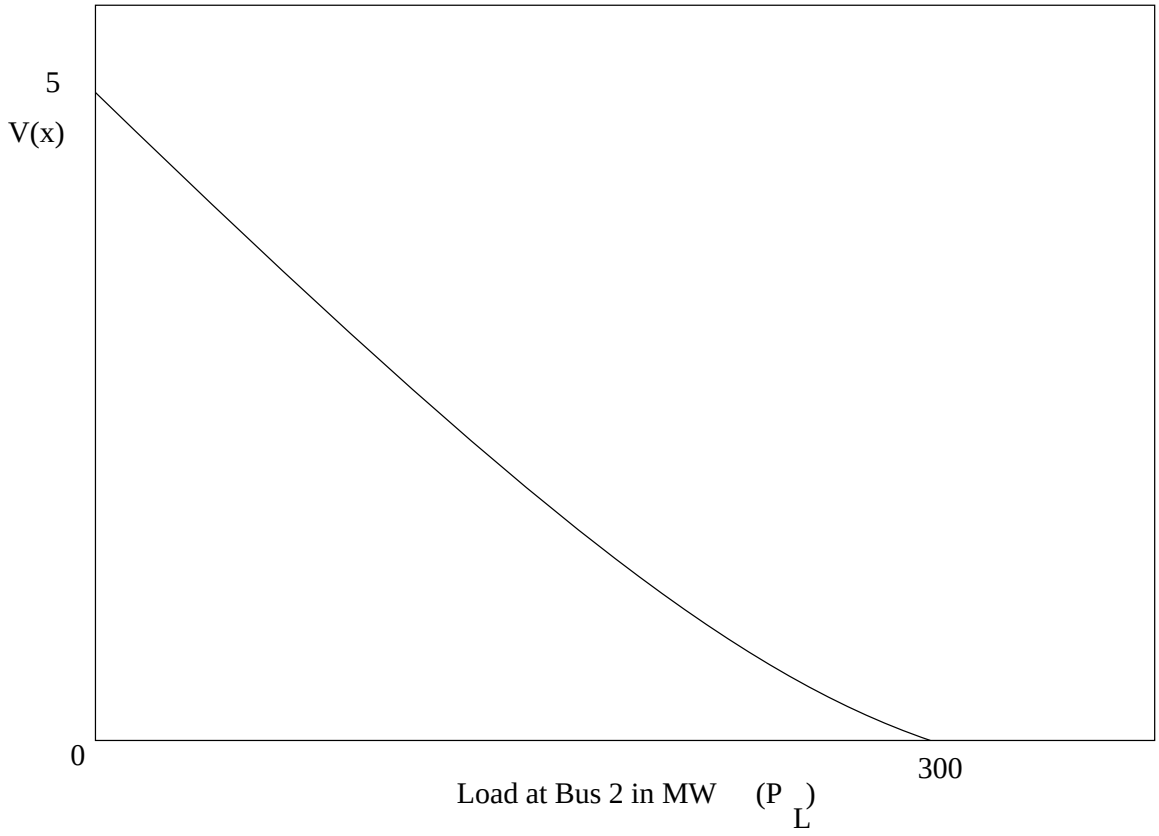

Figure 2.3: Energy function V(x) versus power demand P_L.

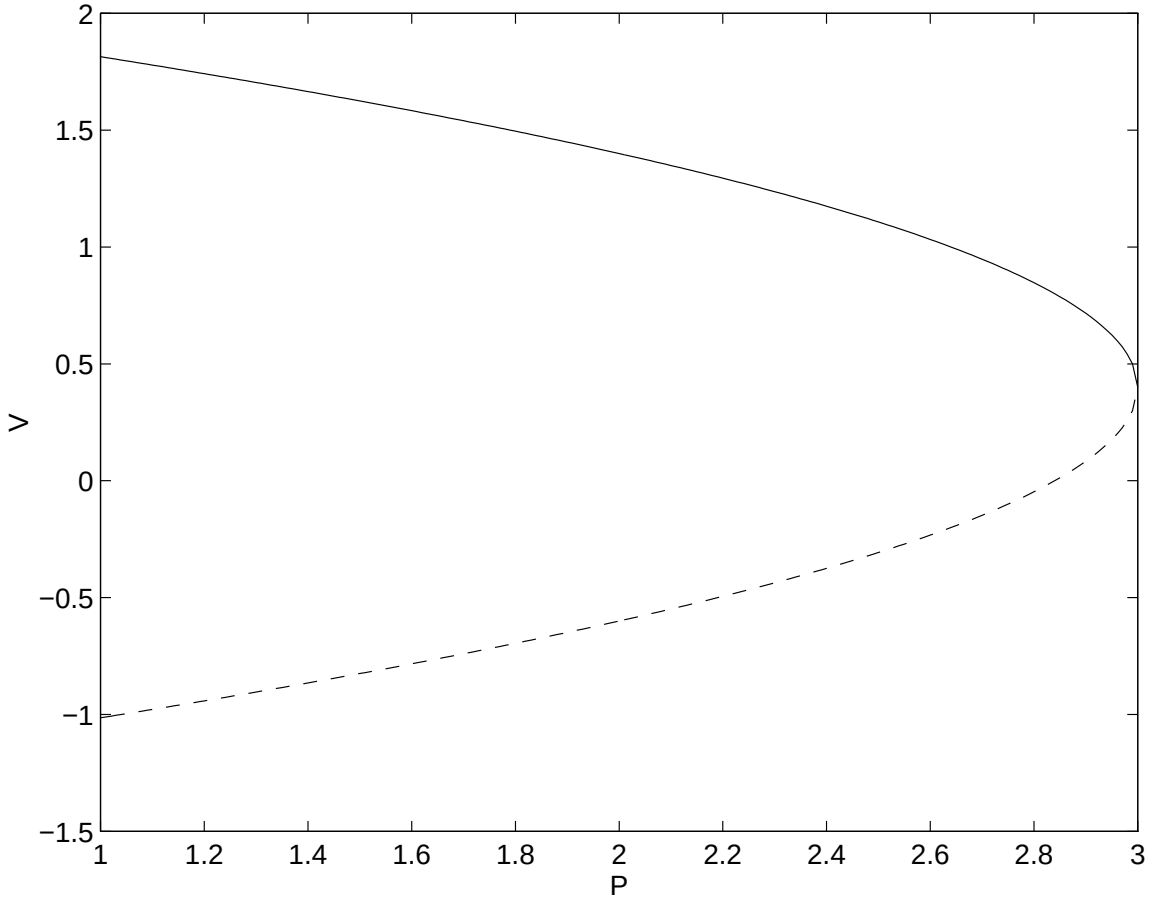

Figure 2.4: V as a Function of P_L.

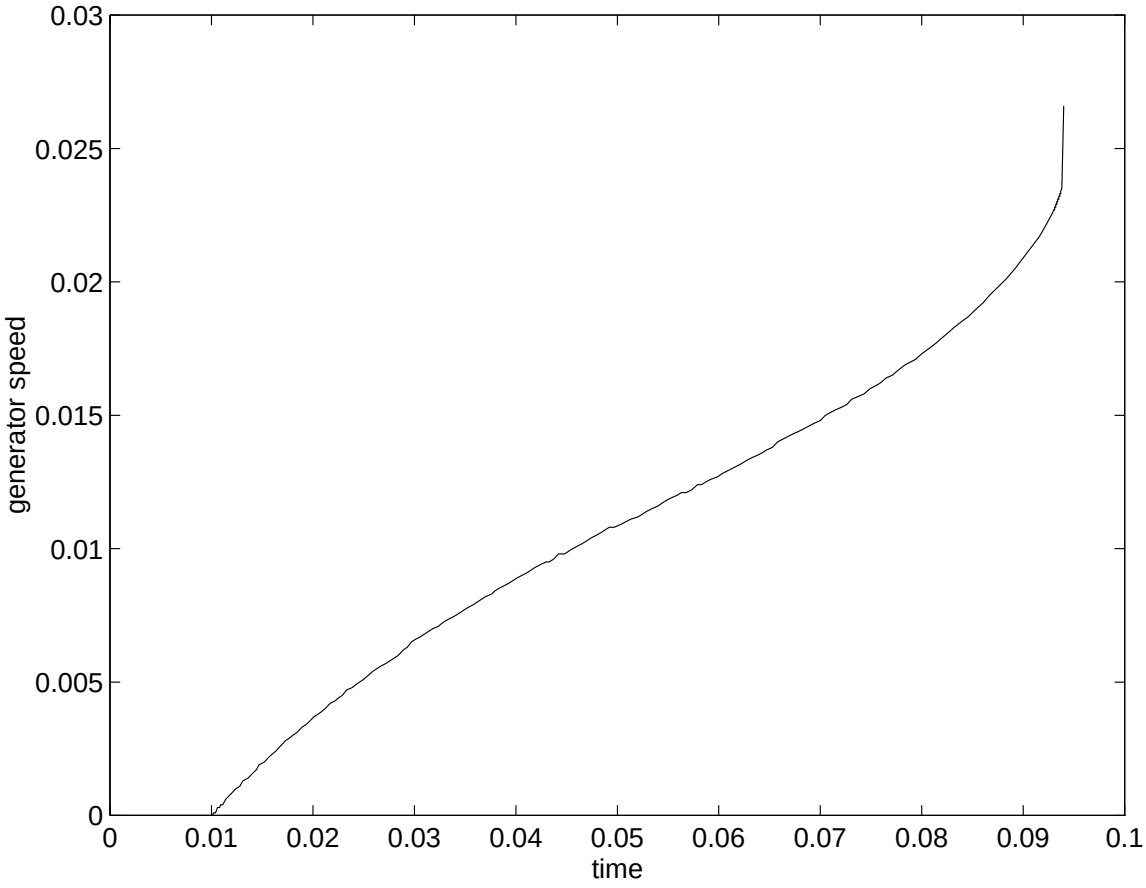

Figure 2.5: Angular generator speed for a load increment beyond the bifurcation value.

stant at 2.9 up to 0.01 seconds, then the load is increased to 3.2. Figures 2.5, 2.6 and 2.7 show the generator angular speed, angular difference between the buses and load bus voltage level with respect to time, respectively. Notice that the system loses stability immediately after the disturbance, resulting in a voltage collapse. For this simulation, $D_g = D_l = M_g = 0.1$, and $T = 0.01$.

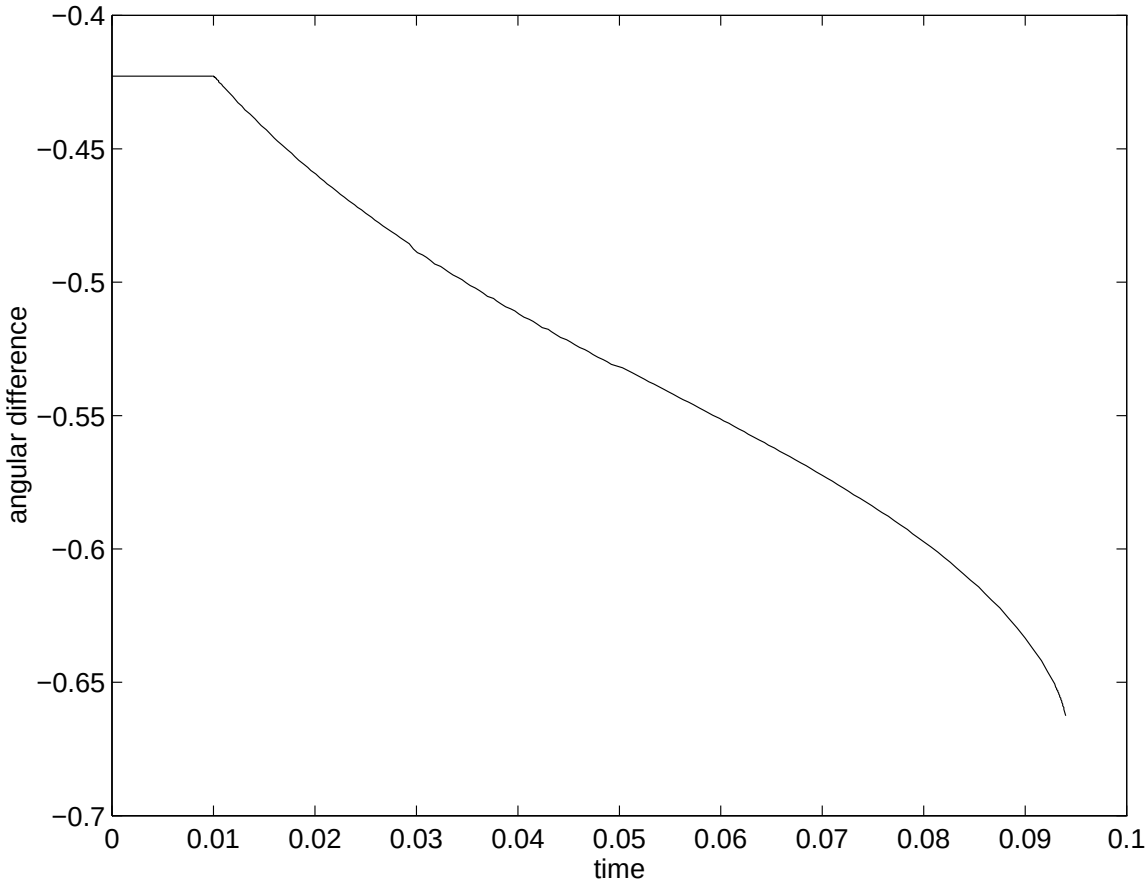

Figure 2.6: Angular difference for a load increment beyond the bifurcation value.

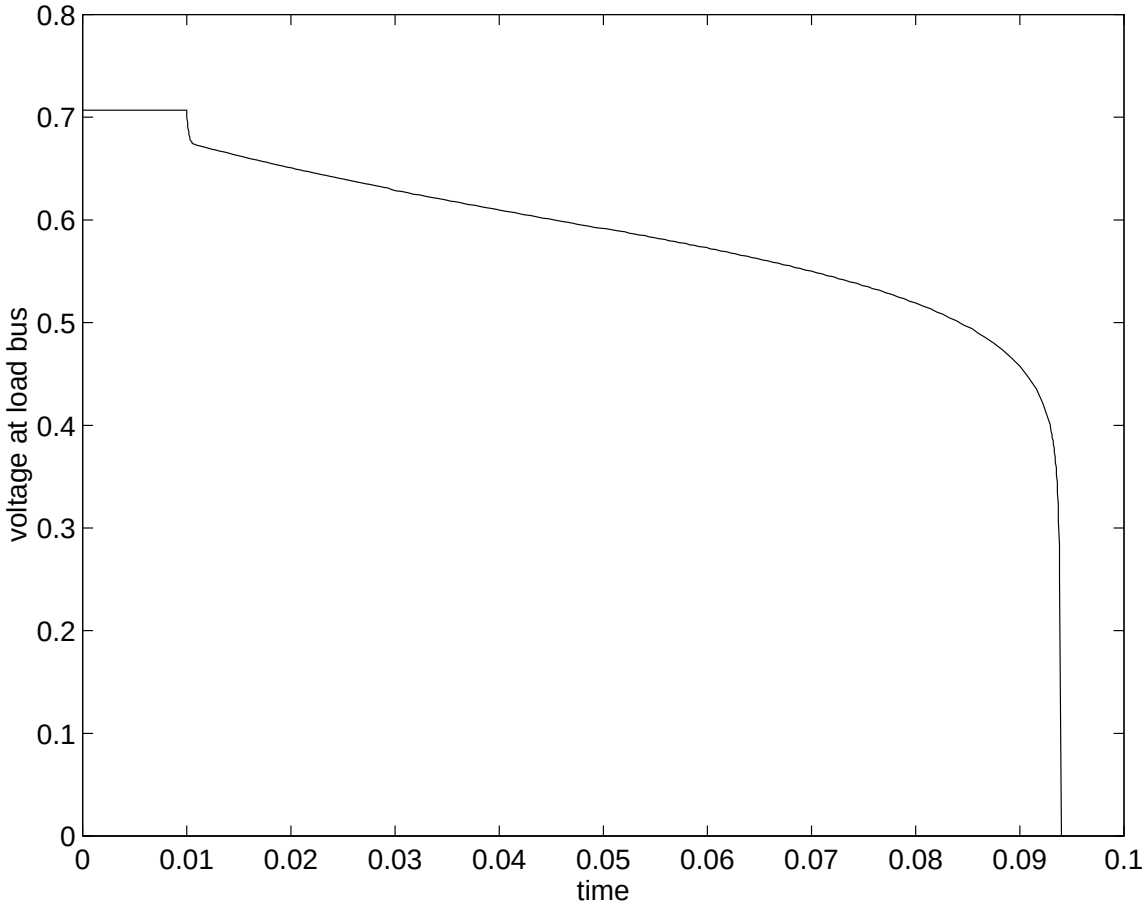

Figure 2.7: Voltage at Bus 2 for a load increment beyond the bifurcation value.

2.3 System Modeling

The energy function derived in the foregoing section helps one understand how successive load increases may lead a system to instability. However, the direct method of Lyapunov may be only applied to certain system models, independent of the perturbation. When analyzing the stability of a system one is interested in the corresponding system model. This model must represent accurately the system under analysis in the time range of interest. Therefore, one is interested in a model that under certain assumptions represents the system as close as possible, and whose solution is computationally efficient. The next sections discusses some load and generator models that appropriately represent the system for static voltage collapse studies.

2.3.1 Load Model

The term "load model" refers to the active and reactive load equations used to represent the load in stability studies. Depending on the computational implementation of these equations in a specific program, the load power or current may or may not be calculated explicitly, but it is useful to think of the model in these terms [44].

1. Static Load Model : A model that expresses the active and reactive powers at any instant of time as functions of the bus voltage magnitude and frequency at the same instant. Static load models are used both for essentially static load components (e.g., resistive and lighting load), and as an approximation for dynamic load components (e.g., motor-driven loads).

   Static Load models are divided as follows:

(a) Constant Impedance load model : A static load model where the power varies directly with the square of the voltage magnitude. It may also be called a constant admittance load model.

(b) Constant Current Load Model : A static load model where the power varies directly with the voltage magnitude.

(c) Constant Power Load Model : A static load model where the power does not vary with changes in voltage magnitude. It may also be called constant MVA load model.

(d) Polynomial Load Model : A static load model that represents the power relationship to voltage magnitude as a polynomial equation, usually in the following form:

$$P = P_o \left[a_1 \left(\frac{V}{V_o} \right)^2 + a_2 \left(\frac{V}{V_o} \right) + a_3 \right]$$

$$Q = Q_o \left[a_4 \left(\frac{V}{V_o} \right)^2 + a_5 \left(\frac{V}{V_o} \right) + a_6 \right]$$

where

- P and $P_o \rightarrow$ Actual and initial active power values.
- a_i for i=1,..,6 $\rightarrow$ Multiplying factors.
- V and $V_o \rightarrow$ Actual and initial voltage level values.
- Q and $Q_o \rightarrow$ Actual and initial reactive power values.

(e) Exponential Load Model - A static load model that represents the power relationship to voltage as an exponential equation, usually in the following form:

$$P = P_o \left(\frac{V}{V_o}\right)^{np}$$

$$Q = Q_o \left(\frac{V}{V_o}\right)^{nq}$$

where

- P and $P_o \rightarrow$ Actual and initial active power values.
- Q and $Q_o \rightarrow$ Actual and initial reactive power values.
- V and $V_o \rightarrow$ Actual and initial voltage level values.
- np and $nq \rightarrow$ Exponential factors.

2. Dynamic Load Model - A model that expresses the active and reactive powers at any instant of time as functions of voltage magnitude and frequency at past instants of time and, usually, including the present instant. Difference or differential equations can be used to represent such models.

Notice that a good load model must be used for voltage collapse analysis, since the distance to a bifurcation point from an operating point may involve a large voltage drop. Such a dynamic load model will be used here, and it has been proposed as [45]:

$$P_L = P_o + P_V \left(\frac{V}{V_o}\right)^{\alpha} + D_L \left(\frac{d\delta}{dt} - \omega_n\right)$$

$$Q_L = Q_o + Q_V \left(\frac{V}{V_o}\right)^{\beta} + T \frac{dV}{dt}$$

where

- $P_L \rightarrow$ Actual active power load for the current operating point
- $P_o \rightarrow$ Portion of constant active power load.
- V and $V_o \rightarrow$ Actual and initial voltage levels
- $P_V \rightarrow$ Initial value of the active power load considering voltage level variation.
- $Q_L \rightarrow$ Actual reactive power load.
- $Q_o \rightarrow$ Portion of constant reactive power load.
- $Q_V \rightarrow$ Initial value of the reactive power load considering voltage level variation.
- $T \rightarrow$ Voltage time constant.
- $D_L \rightarrow$ Load damping.
- $\delta \rightarrow$ Phase angle of load bus.
- β and $\alpha \rightarrow$ Exponential factors.
- $\omega_n \rightarrow$ reference generator speed.

2.3.2 Synchronous Machine Model

Synchronous machine models have been studied for transient stability analysis. For that purpose, the dynamic characteristics of a synchronous machine are represented by several models [22, 32], and the model is chosen either according to available data or computational requirements. For a load-flow analysis, a machine model that assumes a constant terminal voltage has been used when reactive power generation

limits are not violated. For voltage collapse analysis, a model that accurately considers the field and armature limits of a synchronous machine should be considered, as shown in reference [46]. However, in this work the model proposed in [17] is used for simplicity, i.e., the internal generator reactances are neglected and the terminal voltage is assumed constant.

$$\dot{\delta}_g = \omega_g - \omega_n$$

$$\dot{\omega}_g = \frac{1}{M_g}(P_m - P_g - D_g\omega_g)$$

$$P_g = V_g \sum_{k=1}^{n} V_k(G_{gk}\cos(\theta_{gk}) + B_{gk}\sin(\theta_{gk}))$$

$$Q_g = V_g \sum_{k=1}^{n} V_k(G_{gk}\sin(\theta_{gk}) - B_{gk}\cos(\theta_{gk}))$$

where

- $\delta \rightarrow$ Generator phase angle.
- V_g and $V_k \rightarrow$ Voltage magnitude at buses g and k, respectively.
- P_g and $Q_g \rightarrow$ Active and reactive powers delivered by the generator terminals.
- $D_g \rightarrow$ Generator damping.
- $\omega_n \rightarrow$ Reference generator speed, which is assumed to be an infinite bus.
- $\omega_g \rightarrow$ Generator speed.
- $M_g \rightarrow$ Generator inertia.

- $G_{gk} \rightarrow$ Transmission line $g-k$ conductance.
- $B_{gk} \rightarrow$ Transmission line $g-k$ susceptance.
- $\theta_{gk} \rightarrow$ Angular difference between buses g and k.
- $n \rightarrow$ Total number of buses.

In the equations above, the limits in Q_g can be monitored, with the corresponding effect in the overall reactive power generation. When a limit is encountered, the terminal voltage is allowed to vary while Q_g is kept at its limit value.

2.3.3 System Model

The system elements analyzed separately in the two foregoing sections are now considered together to come up with a system model. Although the transmission lines and transformers have not been mentioned, a π-equivalent circuit model is employed to represent all the elements. This system may be represented by a set of differential equations of the form

$$\dot{x} = f(x, \lambda)$$

where $f(x, \lambda)$ represents the active and reactive power mismatches.

Assuming that the system moves slowly from one (s.e.p.) to another as the load is slowly changed, until the bifurcation point is encountered, one can say that static analysis suffices to study the system stability. This model implies that the terminal voltage at the generators is held constant, simulating some of the effects of an AVR.

The model above allows one to detect saddle-node bifurcations using the power flow equations, i.e., $f(x, \lambda) = 0$ [16, 17]. Each operating point has an associated matrix Jacobian, and this matrix allows one to analyze the system behavior around the operating point. Such behavior is studied through small signal perturbation analysis using eigenvalues or singular values decomposition [38, 43]. When a zero eigenvalue or singular value is encountered, a saddle-node bifurcation point is uniquely identified [47].

This system model choice resolves, for this thesis, the discussion about dynamic versus static analysis, since the assumptions made in this section lead one to consider only the load-flow equations for identification of actual saddle-node bifurcations of the corresponding dynamic model [17].

Chapter 3

BIFURCATION AND MATRIX DECOMPOSITION

3.1 Introduction

Identification of a voltage collapse point in a power system has been broadly discussed in the recent literature. The association of this point to a singular Jacobian, as demonstrated in the previous chapter, has provided important tools for voltage collapse investigation. Since the singularity is associated with a zero eigenvalue or a zero singular value, references [38, 43] have developed monitoring methods based on the variation of the smallest eigenvalue and singular value, respectively, in relation to load increase. Such methods have also been exploited in references [31, 48, 49]. In [50, 51] the authors propose performance indices to detect proximity to voltage collapse. Reference [50] proposes the reduction of the load flow Jacobian with respect to a critical bus, while reference [51] proposes a test function. Both techniques yield similar results as discussed in this chapter.

References [12, 19, 45, 52, 53] show that bifurcation theory is useful in the identification of the point of collapse. Different kinds of bifurcation may be encountered in power systems, depending on the system model used.

This chapter discusses typical bifurcations and concentrates in the ones that are possible to identify with the power-flow model used in this thesis. The identification methods proposed in references [38, 43, 50, 51] are also presented.

3.2 Bifurcations in Power Systems

Bifurcations may arise in power systems when the dynamic behavior of a system is changed due to a parameter variation [54]. This section describes four kinds of local bifurcations and the possibility of encountering them in a power system.

A bifurcation point can be defined based on:

$$\dot{x} = f(x, \lambda)$$

where λ is a scalar parameter. The system model described in Chapter 2 fits the equation above. For this system, for each value of λ the state x of the system varies, and the following kinds of bifurcations may be found [7, 54, 55]:

1. Saddle-Node Bifurcation

   This kind of bifurcation may be locally described by the equation

   $$\dot{x} = -x^2 - \lambda$$

   The equilibrium points of the equation above form a parabola which just exists for $\lambda \geq 0$. For $\lambda > 0$ two equilibrium points may be found: $+\sqrt{\lambda}$, which is the

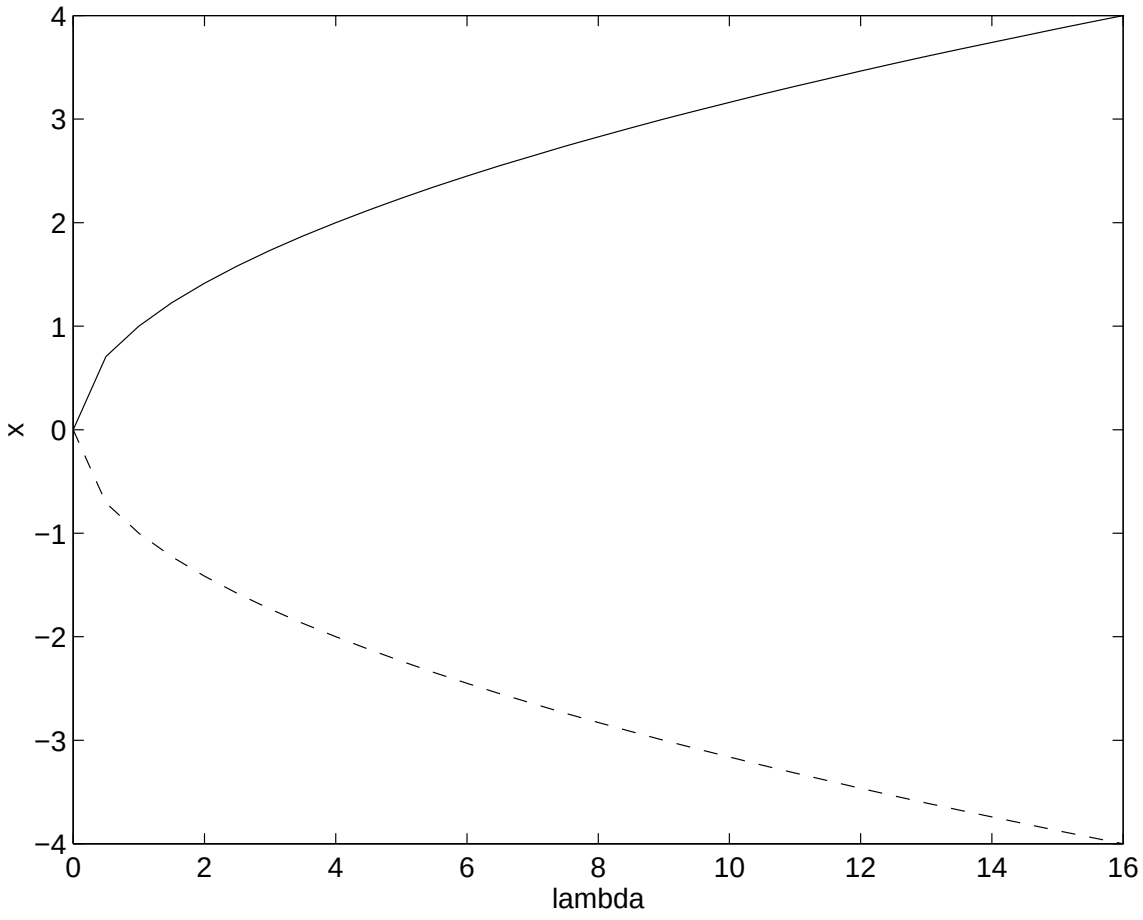

Figure 3.1: Saddle-Node Bifurcation Diagram.

stable equilibrium point, and $-\sqrt{\lambda}$, the unstable equilibrium point. For $\lambda = 0$ only one solution exists, that is the bifurcation point. Figure 3.1 shows the bifurcation phenomenon. The solid line represents the stable branch and the dashed line represents the unstable branch. At the bifurcation point $(0, 0)$, the system eigenvalue is zero. References [17, 25, 45] show that this kind of bifurcation is generic, i.e., it may be found in power systems under typical operating conditions and modeling assumptions.

2. Transcritical Bifurcation

   This type of bifurcation may be locally described by the equation

$$\dot{x} = \lambda x - x^2$$

   The equilibrium points of the equation above are 0 and λ. Figure 3.2 shows the plot of x as a function of λ, and again, the solid line represents the stable equilibrium points and the dashed line represents the unstable equilibrium points. Notice that at $\lambda = 0$ there is an exchange of stability, and the system has a zero eigenvalue. Reference [47] shows that under certain system model conditions, this kind of bifurcation may be detected in power systems.

3. Pitchfork Bifurcation

   Two kinds of pitchfork bifurcation may be identified. The first one is described by the equation below and it is called a Supercritical Pitchfork:

$$\dot{x} = \lambda x - x^3$$

   The equilibrium points for this equation are $x = 0$ and $x = \pm\sqrt{\lambda}$, for $\lambda > 0$. Therefore, the equilibrium points may be plotted as shown in Figure 3.3.

   The other kind of pitchfork bifurcation may be described by the equation below and it is called a Subcritical Pitchfork:

$$\dot{x} = \lambda x + x^3$$

   The equilibrium points for the equation above are given by $x = 0$ and $x = \pm\sqrt{-\lambda}$; therefore, the parabola just exists for $\lambda < 0$. Notice that equilibrium

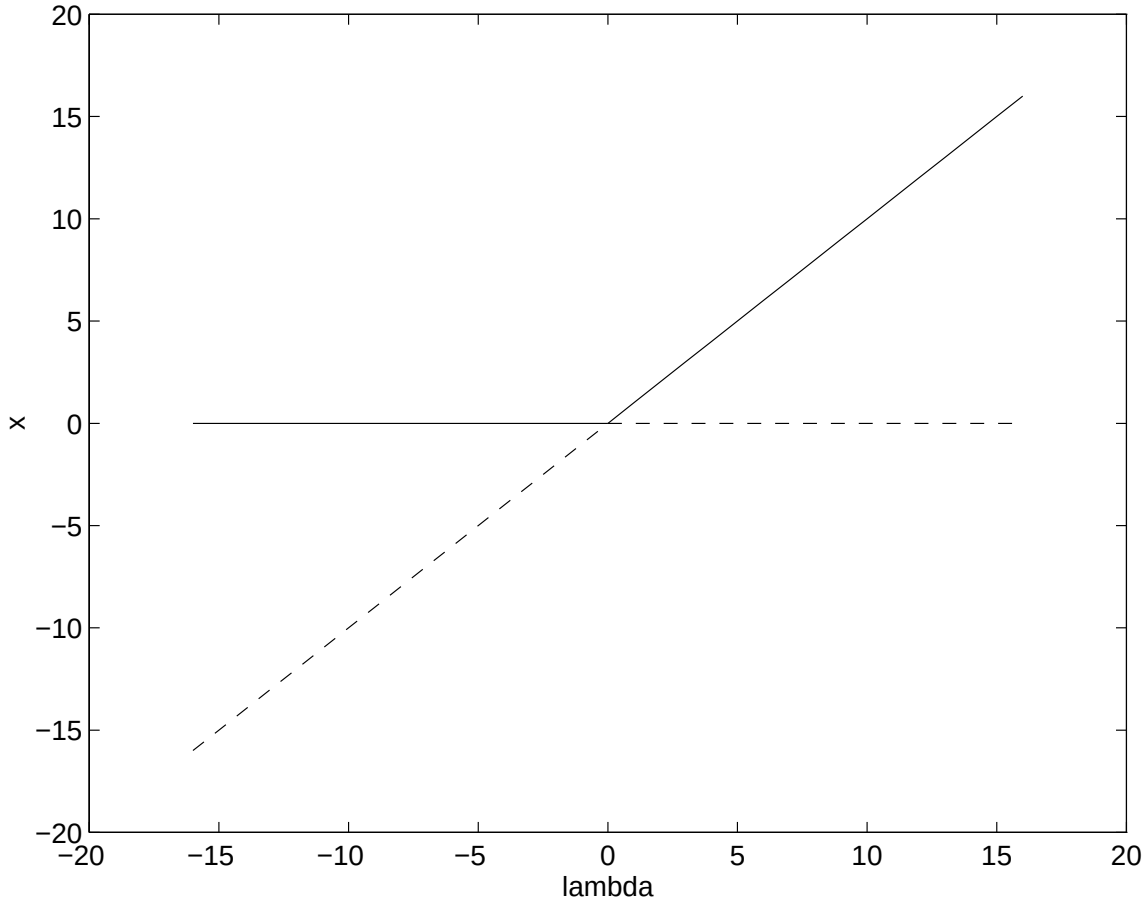

Figure 3.2: Transcritical Bifurcation Diagram.

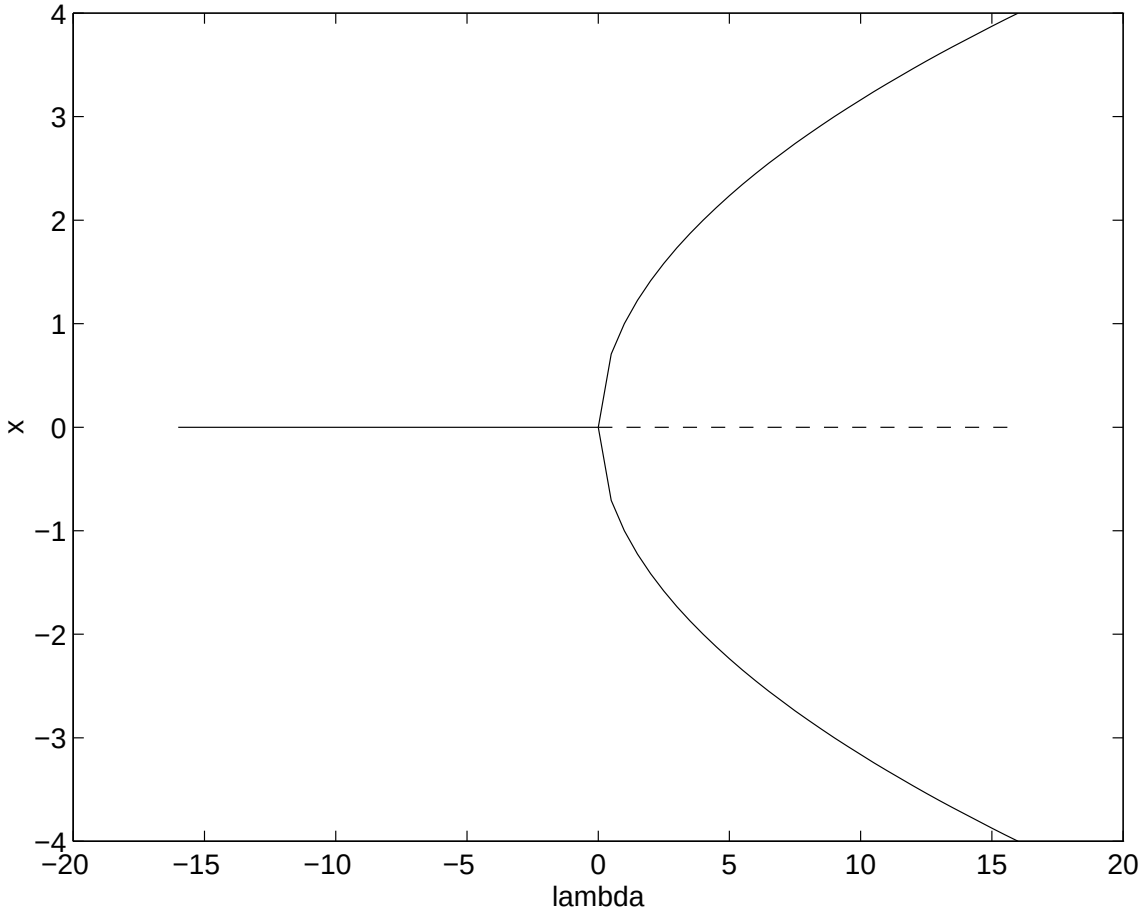

Figure 3.3: Supercritical Pitchfork Diagram.

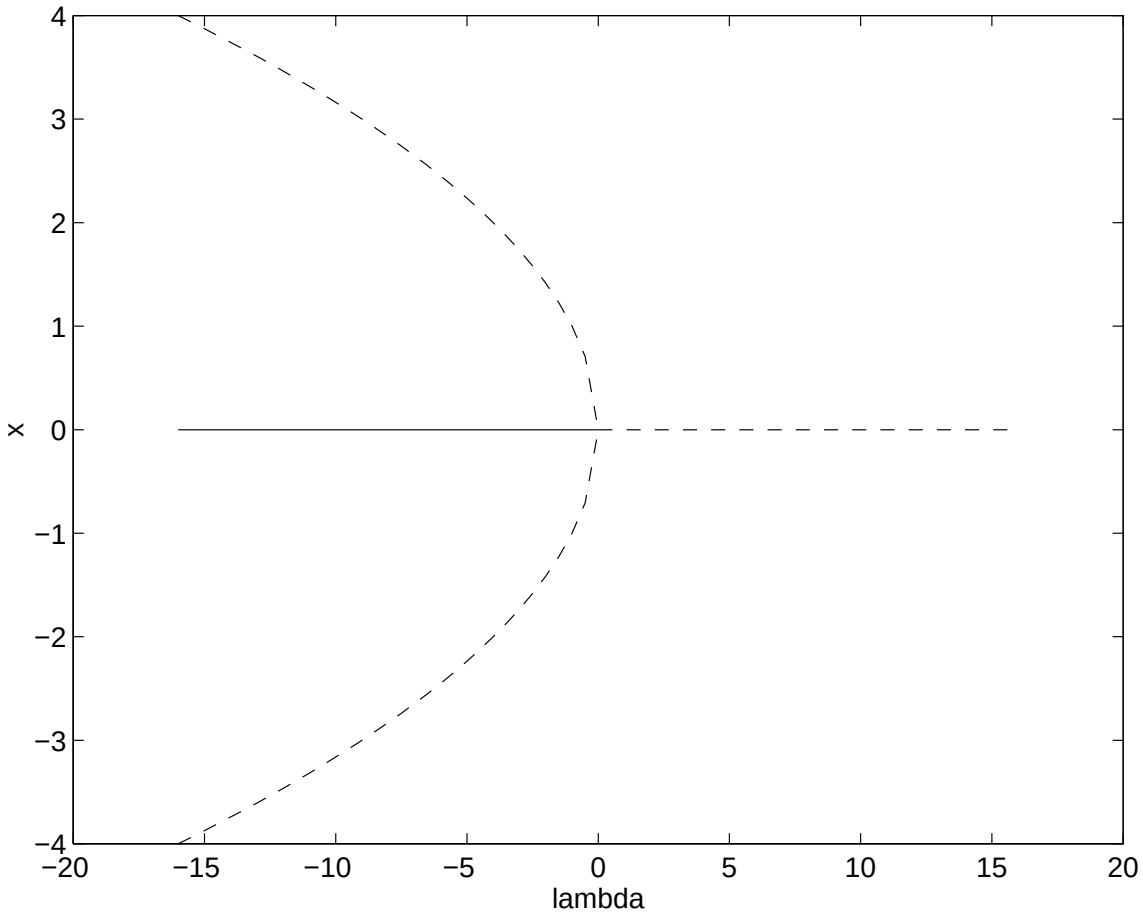

Figure 3.4: Subcritical Pitchfork Bifurcation Diagram.

points given by $\pm\sqrt{-\lambda}$ generate an unstable branch. Figure 3.4 shows the plot of the equilibrium points as a function of λ.

Transcritical and pitchfork bifurcations are non-generic, i.e., they are not expected to take place under typical operating conditions and modeling assumptions. Reference [47] shows that these bifurcations can occur when the system presents a special symmetry due to certain modeling assumptions.

4. Hopf Bifurcation

   This kind of bifurcation does not exist for certain power system models [56]. Hopf bifurcation is identified by a pair of imaginary eigenvalues of the dynamic Jacobian crossing the real axis with non-zero speed [47, 54]. Therefore, this kind of bifurcation cannot be identified with the load flow Jacobian, as the load flow and the dynamic Jacobians are not singular. Two methods to identify this bifurcation point as well as the computational time requirements are discussed in [47]. This issue, however, is beyond the scope of this thesis.

3.2.1 Transversality Conditions of Bifurcations

So far, the definitions of "singular" local bifurcations have been introduced. One is then interested in mathematically distinguishing the characteristics of each bifurcation. Reference [54] analyzes this issue through the determination of the critical points of a set of nonlinear equations

$$0 = f(x, \lambda)$$

Assume that the singular points of these equations correspond to a saddle-node, a transcritical or a pitchfork bifurcation, characterized by a singular system Jacobian of dimension $n \times n$. If the vector of partial derivatives with respect to the parameter λ is attached to the Jacobian matrix, the Jacobian matrix for pitchfork and transcritical bifurcations is singular (rank n-1), while the Jacobian matrix for a saddle-node bifurcation point has rank n (non-singular).

This difference between these kinds of bifurcation may be exploited in the following way: Initially, x is a vector with n components. Including the parameter λ

into the $(n+1)st$ component of x and considering equation $f(x,\lambda)=0$ as a set of n equations in $n+1$ unknowns, the rectangular matrix of the partial derivatives consists of $n+1$ columns. This characteristic allows one to interpret any of the $n+1$ components as a parameter. Such a parameter may be removed from the system Jacobian, yielding a new Jacobian. For a saddle-node bifurcation, if the element associated to the largest entry of the right-zero-eigenvector is removed, the new Jacobian matrix is not singular. However, for the other types of bifurcations, there is no element whose removal from the system Jacobian creates a new non-singular matrix.

The characteristic described above is like rotating the branch diagram x-versus-λ by 90 degrees. This feature is important for continuation methods, which will be discussed in the next chapter.

Now, the transversality conditions of a saddle-node and the other kinds of singular bifurcations may be given as follows:

– Saddle-Node Bifurcation

Condition 1

$f_x(x_0,\lambda_0)$ has a unique & simple eigenvalue 0 with right eigenvector v and left eigenvector w, i.e.,

$$D_x f|_0^T\, w \;=\; D_x f|_0\, v \;=\; 0$$

Condition 2

$$w^T \left.\frac{df}{d\lambda}\right|_0 \neq 0$$

Condition 3

$$w^T \left[D_x^2 f|_0 \, v \right] v \neq 0$$

Conditions 2 and 3 above characterize this kind of bifurcation. They allow to locally transform the bifurcation into $\dot{x} = x^2 \pm \lambda$ around (x_0, λ_0). Such a transformation is known as the Lyapunov-Schimidt reduction [52].

– Transcritical Bifurcation

Condition 1

$f_x(x_0, \lambda_0)$ has a unique & simple eigenvalue 0 with a right eigenvector v and a left eigenvector w, i.e.,

$$D_x f|_0^T \, w = D_x f|_0 \, v = 0$$

Condition 2

$$\omega^T \left[\frac{\partial^2 f}{\partial \lambda \, \partial x}\Big|_0 \right] v \neq 0$$

Condition 3

$$\omega^T \left[D_x^2 f|_0 \, v \right] v \neq 0$$

– Pitchfork Bifurcation

Condition 1

$f_x(x_0, \lambda_0)$ has a unique & simple eigenvalue 0 with a right eigenvector v and a left eigenvector w, i.e.,

$$D_x f|_0^T \, w = D_x f|_0 \, v = 0$$

Condition 2

$$\omega^T \left[\frac{\partial^2 f}{\partial \lambda \, \partial x}\Big|_0 \right] v \neq 0$$

Condition 3

$$w^T \left[D_x^2 f|_0 \, v \right] v = 0$$

Again, these conditions allow to locally transform the system at the bifurcation point (x_o, λ_o) to the standard forms described previously.

3.3 Another View of a Saddle-Node Bifurcation in a Simple Two-Bus System

In this section a simple two-bus system is used to study voltage collapse conditions from a different point of view. The aim of this section is to identify the saddle-node bifurcation described in the previous section in a simple power system, when no limits are considered. Unlike the lossless system shown in Figure 2.2, a more generic transmission line is used. Since no limits are considered, the load may be always supplied by the generator, and the only limiting factor is the transmission line that connects them.

The transmission line series impedance is $|Z| \angle \beta = 0.21 \angle 75^o$ pu. The voltage at bus 2 $V_2 \angle \delta_2$, is unknown, and the voltage at bus 1 is fixed at $V_1 \angle \delta_1 = 1 \angle 0^o$. Then, setting

$$\dot{\delta_1} = \dot{\omega} = \dot{V_2} = 0$$

the dynamic set of equations (2.5) to (2.6) is transformed into the load flow equations, as shown in Chapter 2. The load flow Jacobian, is represented by the partial derivatives of the load bus power equations. Assuming P_L and Q_L as the load at Bus 2 (known values), one has:

$$P_L = \frac{-V_2 V_1}{Z} \cos(\delta_2 - \delta_1 + \beta) + V_2^2 \frac{\cos(\beta)}{Z}$$

$$Q_L = \frac{-V_2 V_1}{Z} \sin(\delta_2 - \delta_1 + \beta) + V_2^2 \frac{\sin(\beta)}{Z}$$

Replacing V_1 and δ_1, the equations become

$$P_L = \frac{-V_2}{0.21} \sin(\delta_2 + 75^o) + V_2^2 \frac{\cos(75^o)}{0.21}$$

$$Q_L = \frac{-V_2}{0.21} \cos(\delta_2 + 75^o) + V_2^2 \frac{\sin(75^o)}{0.21}$$

Therefore, one is interested in determining V_2 and δ_2 for given values of P_L and Q_L. Notice that for each known value of δ_2, two values of V_2 may be calculated. If the angle δ_2 is changed in the equations above, two plots of V_2 as a function of δ_2 can be obtained, one for the active power mismatch and the other for the reactive power mismatch. For a load (P_L, Q_L), the operating point is defined by the intersection of these curves. Figure 3.5 shows the plot of V_2 as a function of δ_2, for three conditions of load, where $P_1 < P_2 < P_3$ and $Q_1 < Q_2 < Q_3$. The power factor is kept constant for all load levels. The intersections of curves P_1 and Q_1 provide two solutions, where P_1 and Q_1 represent the initial load (P_L, Q_L) of the system. The upper intersection point of these curves is the s.e.p., and the other solution is the u.e.p.

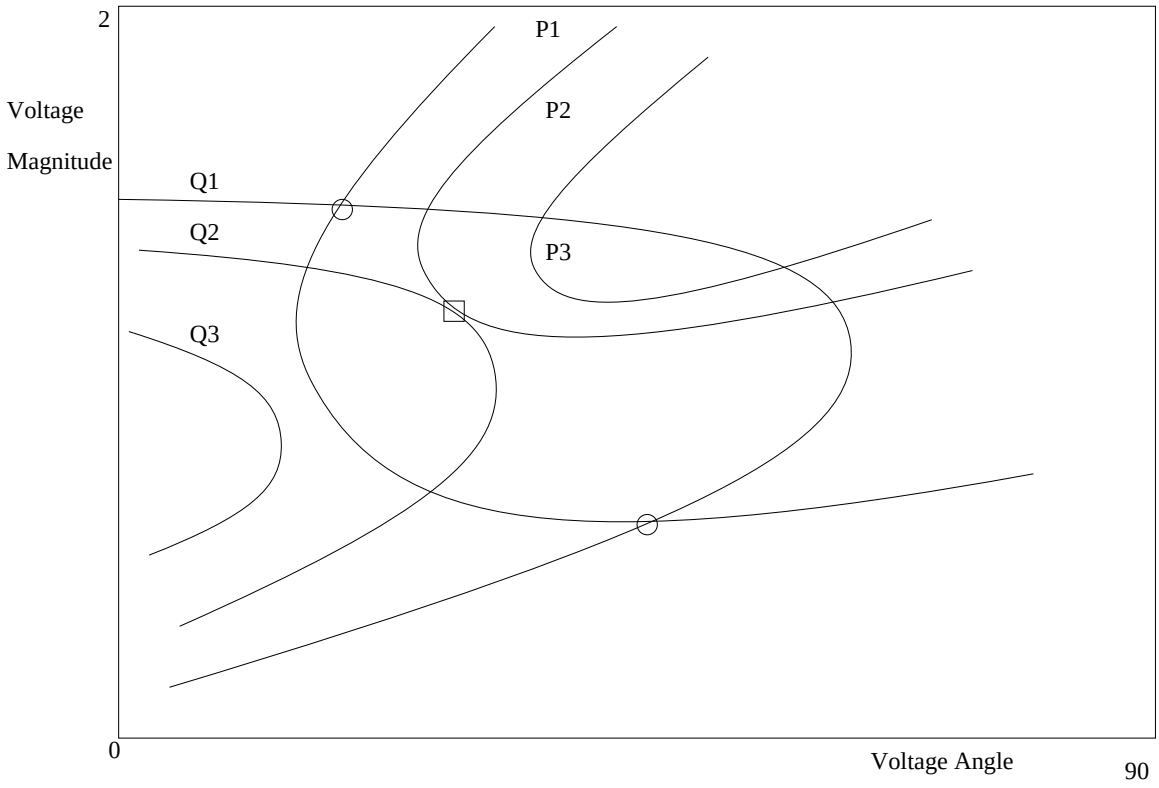

Figure 3.5: Three Possibilities of Load-Flow Solution.

From Figure 3.5, one observes that there is a load level for which only one solution exists, that is indicated by the square in the figure. If the active load demand is increased beyond this point, no solution exists. Since there is no constraint in generation, this power is the maximum flow that the network can transmit [32, 33, 34].

According to Figure 3.5, the load for which a solution is unique provides the boundary between the upper and lower branches of the curves defined by P_2 and Q_2. The fact that one pair of the P and Q curves touch each other at only one point, implies that the gradient vectors ∇P_L and ∇Q_L are aligned. Hence one can write

$$\nabla P_2 - \gamma \nabla Q_2 = 0$$

or equivalently

$$\frac{\partial P_2}{\partial \delta_2} - \gamma \frac{\partial Q_2}{\partial \delta_2} = 0$$

and

$$\frac{\partial P_2}{\partial V_2} - \gamma \frac{\partial Q_2}{\partial V_2} = 0$$

where γ is a scalar number.

The solution of these equations for γ requires that the determinant of the system's Jacobian be equal to zero, i.e.,

$$\left(\frac{\partial P_2}{\partial \delta_2}\right)\left(\frac{\partial Q_2}{\partial V_2}\right) - \left(\frac{\partial P_2}{\partial V_2}\right)\left(\frac{\partial Q_2}{\partial \delta_2}\right) = 0$$

This result means that the Jacobian becomes singular, corresponding to a saddle-node bifurcation, since all transversality conditions apply at this point.

3.4 Extension of Saddle-Node Determination to a Multi-node System

This section extends the saddle-node identification discussed in the foregoing section to a multi-node system, and also presents different methods to identify the critical bus of this system and its proximity to collapse.

3.4.1 Reduced Determinant Calculation

In order to identify the critical bus, an incremental variation ΔP_l and ΔQ_l is assumed at each load bus "l", for $l = 1, \ldots, Npq$, where Npq is the number of load buses in the system. The variations (ΔP_l, ΔQ_l) are taken one at a time while the other load buses have no load variation. The load variation and changing loss are absorbed by the swing bus. This assumption allows one to have no variation in active power generation at PV buses. In a real power system, several generators would share the load increase. Considering these variations and re-ordering the Jacobian, the linearized load flow equations can be written as

$$\begin{bmatrix} 0 \\ 0 \\ \Delta P_l \\ \Delta Q_l \end{bmatrix} = \begin{bmatrix} A & B \\ C & D \end{bmatrix} \begin{bmatrix} \Delta \delta \\ \Delta V \\ \Delta \delta_l \\ \Delta V_l \end{bmatrix} \tag{3.1}$$

The matrix defined by A, B, C, D is the Jacobian J, which is obtained by interchanging rows and columns in the load flow Jacobian so that the bus equations of interest are the last ones. Notice that the 0 elements in the left-hand side of equation (3.1) represent no variations of active power at PV and PQ buses

and reactive power at PQ buses. ΔP_l and ΔQ_l are the assumed incremental load variation at bus l. Therefore, if Npv denotes the number of PV buses and Npq the number of PQ buses, then the involved matrices have the following dimensions

$A : (Npv + 2 * Npq - 2) \times (Npv + 2 * Npq - 2)$,

$B : (Npv + 2 * Npq - 2) \times 2$,

$C : 2 \times (Npv + 2 * Npq - 2)$,

$D : 2 \times 2$

where

- A $\rightarrow$ Partial derivatives of the active power equations in relation to phase angle at all PV buses, and phase angle and voltage level at all PQ buses, but the bus l.
- B $\rightarrow$ Same equations as those of matrix A, but the partial derivatives are derived in relation to phase angle and voltage magnitude at the bus l.
- C $\rightarrow$ Partial derivatives of the active and reactive power equations of the bus l in relation to phase angle at PV buses and phase angle and voltage magnitude at all remaining load buses.
- D $\rightarrow$ Partial derivatives of the active and reactive power equation of the bus l in relation to phase angle and voltage level at the same bus.

Notice that matrices C and D are in the equations of active and reactive powers of the bus of interest; in particular, D stands for those equations that involve the voltage magnitude and phase angle in the bus of interest.

Equations (3.1) can be reduced to

$$\begin{bmatrix} \Delta P_l \\ \Delta Q_l \end{bmatrix} = \begin{bmatrix} D'_l \end{bmatrix} \begin{bmatrix} \Delta \delta_l \\ \Delta V_l \end{bmatrix} \tag{3.2}$$

where

$$D'_l = D - C A^{-1} B \tag{3.3}$$

Matrix D'_l in equation (3.3) can be obtained by a partial factorization of the corresponding load-flow Jacobian J [57]. Furthermore, this matrix is also well defined at all operating points, since A is guaranteed nonsingular even at the collapse point, as long as bus l has non-zero entries in the "zero" eigenvectors of J at the bifurcation point; this is particularly true for $l = c$ (the critical bus), which is identified as the bus with the largest entries in the right-eigenvector. Thus, the determinant of D'_l,

$$\det D'_l = \frac{\det J}{\det A} \tag{3.4}$$

becomes zero only at the bifurcation or collapse point.

Matrix D'_l relates the active and reactive powers of the bus of interest to its voltage magnitude and phase angle, considering implicitly all the other equations of the load flow Jacobian. The bus associated to the smallest D'_l is the critical bus of the system.

Since the determination of the critical bus by this technique requires the calculation of the load flow Jacobian reduction for all load buses, it is rather time consuming for a large power system.

3.4.2 Singular Value Decomposition

Singular values have been employed in power systems because of the useful orthonormal decomposition of the Jacobian matrices. For a real square matrix A of dimension $n \times n$, one has that

$$A = X\Sigma Y^T = \sum_{i=1}^{n} x_i \sigma_i y_i^T$$

where the singular vectors x_i and y_i are the i^{th} columns of the unitary matrices X and Y, and Σ is a diagonal matrix of positive real singular values σ_i, such that $\sigma_1 \geq \sigma_2 \geq .... \geq \sigma_n$. The diagonal entries of Σ^2 correspond to the eigenvalues of matrix AA^T. This singular value decomposition is typically used to determine the rank of a matrix, which is equal to the number of non zero singular values of A [58, 59]. Hence, its application to static voltage collapse analysis focuses on monitoring the smallest singular value up to the point when it becomes zero [43].

In power systems, the matrix A represents the load-flow Jacobian J, which typically contains the first derivatives of active and reactive power mismatch equations, $\Delta P = \Delta P(\delta, V)$ and $\Delta Q = \Delta Q(\delta, V)$, with respect to the voltage magnitude V and angles δ, i.e., the linearization of these equations yields

$$\begin{bmatrix} \Delta P \\ \Delta Q \end{bmatrix} = J \begin{bmatrix} \Delta \delta \\ \Delta V \end{bmatrix} \tag{3.5}$$

Thus, one can rewrite (3.5), at equilibrium points other than the bifurcation point, as

$$\begin{bmatrix} \Delta \delta \\ \Delta V \end{bmatrix} = X\,\Sigma^{-1}\,Y^T \begin{bmatrix} \Delta P \\ \Delta Q \end{bmatrix} = \sum_{i=1}^{n} \sigma_i^{-1} x_i y_i^T \begin{bmatrix} \Delta P \\ \Delta Q \end{bmatrix} \tag{3.6}$$

Notice that the minimum singular value is a relative measure of how close the system is to the voltage collapse or singular point. Furthermore, near this bifurca-

tion point, since σ_n is close to zero, equation (3.6) can be rewritten as

$$\begin{bmatrix} \Delta\delta \\ \Delta V \end{bmatrix} \approx \sigma_n^{-1} x_n y_n^T \begin{bmatrix} \Delta P \\ \Delta Q \end{bmatrix}$$

Thus, the associated left and right singular vectors x_n and y_n, respectively, can be interpreted as follows [43]:

1. The maximum entries in x_n indicate the most sensitive voltage magnitudes and angles (critical buses).

2. The maximum entries in y_n correspond to the most sensitive direction for changes of active and reactive power injections.

In [29], the author proposed to reduce the load-flow Jacobian to the first derivative of reactive power equations in relation to voltage magnitude, by assuming that the generator and load buses present no active power variation, i.e., $\Delta P = 0$. Thus,

$$\begin{aligned} \begin{bmatrix} \Delta P \\ \Delta Q \end{bmatrix} &= \begin{bmatrix} J_1 & J_2 \\ J_3 & J_4 \end{bmatrix} \begin{bmatrix} \Delta\delta \\ \Delta V \end{bmatrix} \\ \Rightarrow \quad \Delta Q &= (J_4 - J_3 J_1^{-1} J_2)\Delta V = J_{QV}\Delta V \end{aligned} \tag{3.7}$$

where $J_1 = [\partial P/\partial\delta]$, $J_2 = [\partial P/\partial V]$, $J_3 = [\partial Q/\partial\delta]$, and $J_4 = [\partial Q/\partial V]$. In general, at the saddle-node bifurcation point one has that J_1 is not singular, even though J is singular. There is not definite proof of the latter statement, but in practice that seems to be the case in all examples discussed in the literature and is also the experience of the author of this thesis. Thus, J_{QV} is assumed well defined in (3.7), becoming singular at the bifurcation point since

$$\det J_{QV} = \frac{\det J}{\det J_1}$$

The singular values of this reduced matrix can then be used to determine proximity to voltage collapse. It is interesting to highlight the fact that sub-matrix J_4 is quasi-symmetric, for small values of transmission system resistances. Therefore, one expects a similar attribute for J_{QV} in equation (3.7), making the singular values and eigenvalues practically identical, since symmetric matrices have similar singular value and eigenvalue decomposition [58, 59].

3.4.3 Eigenvalue Decomposition

The authors in [38] apply an eigenvalue decomposition to the reduced load-flow Jacobian J_{QV}. This decomposition for a real square diagonalizable (semi-simple) matrix A can be written as [58]:

$$A = V\Lambda W^T = \sum_{i=1}^{n} v_i \mu_i \omega_i^T$$

where V represents a complex matrix of right eigenvectors v_i, W corresponds to the complex matrix of left eigenvectors ω_i, and Λ is a diagonal matrix of complex eigenvalues μ_i of A.

For the J_{QV} matrix defined in (3.7), this decomposition may be applied directly, since this matrix is quasi-symmetric and, therefore, diagonalizable. Furthermore, due to its quasi-symmetric structure, one expects to obtain a set of only real eigenvalues and eigenvectors, very similar in value to the corresponding singular values and singular vectors. Thus, near the bifurcation or voltage collapse point the eigenvectors associated to the eigenvalue closest to zero have the same interpretation as the singular vectors, i.e., the maximum entries in the right eigenvector correspond to the critical buses (most sensitive voltages) in the system, and the maximum entries in the left eigenvector pinpoints the most sensitive direction for changes of

power injections [8, 38]. It is the observation of the authors that as the size of the system increases, the singular values and absolute eigenvalues become closer.

3.4.4 Test Functions

Seydel in [54] discusses a family of scalar test functions t_{lk} defined as

$$t_{lk} = e_l^T J J_{lk}^{-1} e_l \tag{3.8}$$

where J corresponds to the system Jacobian, and e_l is the l^{th} unit vector, i.e., a vector with all zero entries except for an entry of 1 in row l. The matrix J_{lk} is defined as follows:

$$J_{lk} = (I - e_l e_l^T)J + e_l e_k^T \tag{3.9}$$

where I represents the identity matrix. equation (3.9) can be interpreted simply as an operation on the Jacobian matrix J where the l^{th} row is removed and replaced by the row e_k^T. Notice that for the load-flow equations at the voltage collapse or bifurcation point J is singular, but matrix J_{lk} is guaranteed not singular if the l^{th} and k^{th} are chosen so that they correspond to non zero entries in the "zero" eigenvectors, say vectors v_n and ω_n associated to the zero eigenvalue of J. Furthermore, if $l = k = c$, where c corresponds to the maximum or critical entry in v_n, the test function becomes the "critical" test function

$$t_{cc} = e_c^T J J_{cc}^{-1} e_c \tag{3.10}$$

The authors in [51] use the test function of equation (3.8) to define an index of proximity to collapse. Thus, let's assume that the load-flow vector nonlinear equations are defined as the active and reactive power mismatches at the system

buses

$$\begin{aligned} \Delta P(\delta, V, \lambda) &= 0 \\ \Delta Q(\delta, V, \lambda) &= 0 \end{aligned} \tag{3.11}$$

where V and δ represent the phasor bus voltages, as stated above, and λ represents a scalar parameter or loading factor used to simulate the system load changes that drive the system to collapse in the following way:

$$P_l = P_{l_P}(1 + \lambda)$$

$$Q_l = Q_{l_Q}(1 + \lambda)$$

Here P_l and Q_l represent the load at bus l, and P_{l_P} and Q_{l_Q}, are all pre-defined constants that determine the load model [45]. Hence, the Jacobian matrices and test function family become functions of the system variables and parameter, i.e., for $z = [\delta^T \; V^T]^T$, $J = J(z, \lambda)$, $J_{lk} = J_{lk}(z, \lambda)$, and $t_{lk} = t_{lk}(z, \lambda)$. As the parameter λ changes approaching bifurcation, the system variables change, with the critical test function t_{cc} displaying a quadratic or quartic shape [51], i.e,

$$t_{cc}(z, \lambda) \approx a\Delta\lambda^{1/c}$$

where a is a scalar constant, c is either 2 (quadratic) or 4 (quartic), and $\Delta\lambda = \lambda - \lambda_0$ (λ_0 is the maximum loading factor, i.e., the bifurcation value of the system parameter). In general, test functions t_{lk} for buses other than the critical bus c do not display this particular shape. Based on this approximation of t_{cc}, the index of proximity to collapse is defined in [51] as

$$\tau = -\frac{1}{c}\frac{t_{cc}(z, \lambda)}{\frac{dt_{cc}}{d\lambda}(z, \lambda)} \tag{3.12}$$

This index τ presents in some cases a linear behavior with respect to changes in the loading factor λ, as illustrated in [51]. However, when limits are considered t_{cc} does not exhibit an overall quadratic or quartic shape. Another difficult with τ is the problem determining the critical bus c. This can be pinpointed from the maximum entries in the vector $\frac{dz}{d\lambda}$ at an operating point (z_1, λ_1) [36, 53], where

$$\frac{dz}{d\lambda} = J^{-1} \begin{bmatrix} \left.\frac{\partial \Delta P}{\partial \lambda}\right|_1 \\ \\ \left.\frac{\partial \Delta Q}{\partial \lambda}\right|_1 \end{bmatrix}$$

since this "tangent" vector converges to the "zero" right eigenvector x_n at the bifurcation point [25, 19].

Notice that the load-flow Jacobian J is a particular case of $D_x f|_0$. Therefore, the techniques proposed here to identify saddle-node bifurcations in power systems may be extended to any set of nonlinear equations.

However, in general, one needs to be rather close to the bifurcation point to accurately estimate this bus, as demonstrated in Chapter 5 of this thesis for a 300-bus system.

Chapter 4

LOAD MARGIN DETERMINATION

4.1 Introduction

Load margin determination of a power system with respect to a bifurcation point plays a very important role on voltage collapse analysis. Reference [29] proposes a Lagrangian function for the net reactive power injections into the buses of a power system to determine this margin. References [34, 38, 39, 43, 51] propose other methods to evaluate the load margin; however, none of these techniques allows one to trace the bifurcation manifold.

References [25, 36] show that continuation methods not only identify the load margin properly, but also trace the bifurcation manifold. Such methods provide accurate results; however the computational time required for a large system is still a barrier for their application. Direct methods may also identify the bifurcation point [25, 36, 54], but since they use iterative methods, a good initial guess is

required, otherwise the convergence may not be obtained. Unlike continuation methods, these methods do not trace the bifurcation manifold.

Computational time may be improved if the number of equations is reduced, as shown in [32, 36]. This reduction may be obtained either through the elimination of a certain set of equations or a network partitioning technique.

In this chapter, direct and continuation methods are described. In order to reduce the computational burden, network partitioning and reduction are presented using different techniques.

4.2 Direct Method

This technique, also known as the "point of collapse method", was developed to find saddle-node bifurcations of nonlinear systems. For a known operating point, the idea is to find the distance (load margin) to a singular bifurcation by the Newton-Raphson method [25, 54]. The initial set of equilibrium equations $f(x, \lambda) = 0$ is enlarged as follows:

$$\begin{aligned} f(x,\lambda) &= 0 \\ D_x f(x,\lambda) v &= 0 \\ \|v\| &\neq 0 \end{aligned} \tag{4.1}$$

or

$$\begin{aligned} f(x,\lambda) &= 0 \\ D_x^T f(x,\lambda) \omega &= 0 \\ \|\omega\| &\neq 0 \end{aligned} \tag{4.2}$$

where

- $f(x, \lambda) = 0 \rightarrow$ bifurcation manifold. This subset has dimension n.
- $D_x f(x, \lambda)v = 0$ or $D_x^T f(x, \lambda)\omega = 0 \rightarrow$ singularity condition of Jacobian $D_x f(x, \lambda)$. This subset has dimension n.
- $\|v\|$ or $\|\omega\| \rightarrow$ nonzero eigenvector norm, with dimension 1.

Therefore, the whole set of equations (4.1) or (4.2) has dimension $2n + 1$.

Notice that since the Jacobian $D_x f(x, \lambda)$ is singular at the bifurcation point, a nonsingular eigenvector v or ω must be guaranteed. This set of equations may have several solutions, and since a Newton-Raphson method is employed, a good initial guess is required to find the desired solution. Reference [54] proposes a method to guess the initial v or ω, based on a manipulation of the Jacobian $D_x f(x, \lambda)$. Another way of guessing the initial v or ω is finding such vectors for the initial operating point.

If the initial operating point is far from the bifurcation point, several limits may be reached during the process, such as reactive power generation or transformer taps. These limits change the structure of $f(x, \lambda)$ and its Jacobian. If the limits of the system are neglected, the solution process is faster, although not realistic.

An important issue regarding load margin determination is the direction of load increase, since a different bifurcation point may be calculated for each load direction.

4.3 Continuation Method [53]

Like the direct method, this technique is used to find bifurcations of nonlinear equations. An advantage of this method is that it does not only find bifurcations,

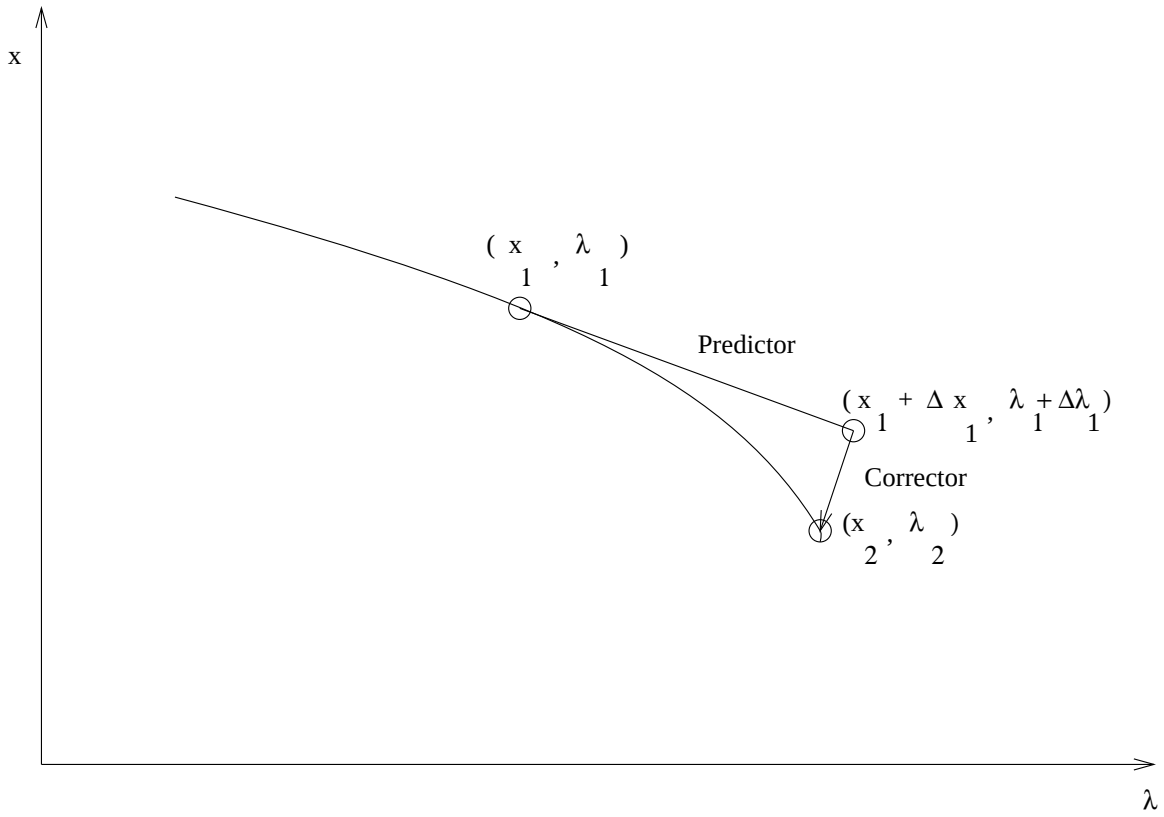

Figure 4.1: Continuation method process.

but also traces the bifurcation manifold, yielding accurate results. The method is divided in two steps, to trace the manifold $f(x, \lambda) = 0$ starting at the equilibrium point (x_1, λ_1)

1. Predictor: Assuming that the initial operating point (x_1, λ_1) is known, one has

$$f(x_1, \lambda_1) = 0$$

the partial derivatives with respect to x and λ yields

$$D_x f(x_1, \lambda_1)\frac{dx_1}{d\lambda} + \frac{\partial f(x_1, \lambda)}{\partial \lambda} = 0$$

Thus, the tangent vector is given at that point by

$$t_1 = \frac{dx}{d\lambda} = -D_x^{-1} f(x_1, \lambda_1)\frac{\partial f(x_1, \lambda_1)}{\partial \lambda} \tag{4.3}$$

where $D_x f(x_1, \lambda_1)$ represents the load-flow Jacobian.

As the system approaches the bifurcation, the system matrix Jacobian becomes ill-conditioned, and the tangent vector may not be defined. Therefore, parameterization can be used to avoid this problem.

Step Length Control

The step generated by the predictor is given by:

$$\frac{\Delta x_1}{\Delta \lambda_1} = t_1 \tag{4.4}$$

Hence, one can choose

$$\Delta \lambda_1 = \frac{k}{\|t_1\|}$$

to normalize the size of the step, where k is a constant value. For $k = 1$, the process has a "normal" tracing, and for $k > 1$ or $k < 1$ it provides fast or slow tracing, respectively. This expression for $\Delta \lambda_1$ yields

$$\Delta x_1 = k\frac{t_1}{\|t_1\|}$$

Therefore, as steeper is the curve, the smaller is the step length.

2. Corrector Step

   This step finds the solution (x_2, λ_2) in the bifurcation manifold from point $(x_1+\Delta x_1, \lambda_1+\Delta\lambda_1)$, generated by the predictor step. This solution is obtained solving the set of equations

$$f(x, \lambda) = 0$$

$$\rho(x, \lambda) = 0$$

   which is a set of equations with dimension $(n+1) \times (n+1)$.

   From Figure 4.1, using a vector perpendicular to the tangent vector, one has that

$$\rho(x,\lambda) = \begin{bmatrix} \Delta x_1 \\ \Delta\lambda_1 \end{bmatrix}^T \begin{bmatrix} x_2 - x_1 - \Delta x_1 \\ \lambda_2 - \lambda_1 - \Delta\lambda_1 \end{bmatrix} = 0 \qquad (4.5)$$

   or

$$\rho(x, \lambda) = \Delta x_1(x_2 - x_1 - \Delta x_1) + \Delta\lambda_1(\lambda_2 - \lambda_1 - \Delta\lambda_1) = 0$$

   Starting from the solution provided by the predictor step, the equations above converge to (x_2, λ_2).

   Figure 4.1 clearly illustrates the meaning of the predictor and corrector steps.

4.4 Network Partitioning

4.4.1 General Aspects

Let n be the number of nodes in a network and C_{ij} the connection measure between two nodes i and j. A trivial connection measure C_{ij} is given by the branch value that connects nodes i and j, a known value. For example, one can take a general network formed by a set of highways connecting several cities. C_{ij}, in this case, may be the number of cars that travel from city i to city j (or vice-versa) in a certain instant of time. Therefore, C_{ij} is not constant, and depends directly on the traffic conditions. Similar analysis may be done in power systems, where i and j are nodes (buses). C_{ij} must be determined with respect to load level dependence. Such a definition for partitioning purposes, depends on the technique employed and will be shown in the next sections.

If C_{ij} is large, one can say that node i is strongly connected to node j. Otherwise, nodes i and j are said to be weakly connected. A set of nodes strongly connected to each other is called a block. A network partitioning arises from the assumption that if nodes i and j are weakly connected, node i does not play an important role on the analysis of node j, and can be neglected.

Reference [60] proposes an eigenvector-based decomposition technique. By this technique, the partition is given by sorting the right eigenvector associated with the smallest eigenvalue of a connectivity matrix. Reference [61] employs this technique to obtain the initial partition and tries to improve it using an interchange method. This technique is based on the nodes exchanged among the blocks, thus is carried out up to the point when no more improvements are obtained for further interchanges.

For a power system partitioning, the trivial connection between two nodes is represented by the transmission line connecting them. However, this measure does not identify whether two unconnected buses are strongly or weakly tied to each other. Like the highway example cited above, two buses strongly connected for an operating point, may be weakly connected for another system condition. Therefore, it is necessary to come up with a method to calculate C_{ij} for each known operating point.

Calculating C_{ij} in a power system may lead one to analyze a different network, created from the original one. This new network depends on the choice of C_{ij}. Reference [37] calculates C_{ij} as the voltage variation in all load buses j with respect to a load variation in the bus of interest i. References [32, 33, 34] employ the reduced Jacobian determinant, discussed in Chapter 3, to calculate C_{ij}. In this thesis, C_{ij} is defined as the relation between the entry in the vector (of each one of the techniques proposed here) associated to the bus of interest i and the vector component associated to any other bus j.

This section describes several network partitioning techniques.

4.4.2 Partitioning by Right Eigenvector

The idea of a network partitioning by an eigenvector-based technique has been exploited in [60, 61, 62], where clustering techniques are proposed, depending on the desired number of blocks. In this thesis, the number of blocks is not previously defined, but calculated as a function of C_{ij} and a specified value k. Based on the knowledge that the zero-right-eigenvector provides the rank of the critical buses [25], the following technique is proposed:

1. Find the right eigenvector associated to the smallest eigenvalue of a Jacobian matrix for a known operating point.

2. Sort the components of this eigenvector.

3. From the most critical bus (largest entry on the right eigenvector), find an initial critical area with the first neighbors of this bus (level 1).

4. Add new levels of neighboring buses to this basic critical area. For each level, find the relation between the eigenvector component associated to each neighbor bus j and the critical bus i, yielding C_{ij}. The critical area associated to the first critical bus is obtained when the largest C_{ij} is smaller than a specified value k. If this condition is not satisfied, continue adding new levels of neighboring buses and calculate C_{ij}. After finding the critical area associated to the first critical bus, repeat the process from Step 3 for the remaining buses.

The buses that do not belong to the critical area but connect this area to the rest of the system (border buses), are considered as part of the reduced system and treated as constant voltage buses, i.e., PV buses. This is done based on the assumption that their steady-state voltage magnitudes are not significantly affected by the parameter changes in the system.

4.4.3 Partitioning by Tangent Vector

The technique described in the foregoing section depends on the determination of the right eigenvector. Therefore, it is desirable to obtain a technique that requires less computational time. Since the tangent vector converges to the zero right eigenvector at the bifurcation point [25], and it shows how the system variables change

with loading, a partitioning technique based on this tangent vector is proposed in this work. The tangent vector may be obtained by a direct solution, which makes it cheaper than calculating the eigenvector.

For the equilibrium equations,

$$f(x, \lambda) = 0$$

the tangent vector is defined as

$$\frac{dx}{d\lambda} = [D_x f(x, \lambda)]^{-1} \frac{\partial f}{\partial \lambda}$$

where $J = D_x f(x, \lambda)$ if the load flow equations are used.

The four-steps partitioning proposed in the foregoing section is then used with the tangent vector instead of the right eigenvector.

4.4.4 Partitioning by Reduced Jacobian Determinant

The two methods proposed in this section are based on the changes of voltage level at the initial critical bus, with variations of the active and reactive power loads at the remaining load buses [34]. Thus, for each load bus, it is known from equation (3.2) that

$$\begin{bmatrix} \Delta P_l \\ \Delta Q_l \end{bmatrix} = \begin{bmatrix} D'_l \end{bmatrix} \begin{bmatrix} \Delta \delta_l \\ \Delta V_l \end{bmatrix}$$

Hence,

$$\begin{bmatrix} \Delta\,\delta l \\ \Delta\,V_l \end{bmatrix} = \begin{bmatrix} L \end{bmatrix} \begin{bmatrix} \Delta\,P_l \\ \Delta\,Q_l \end{bmatrix} \tag{4.6}$$

where $L = D_l'^{-1}$. Notice that L has the same dimension as D_l', i.e., 2x2.

Lets assume that

$$L = \begin{bmatrix} E & F \\ G & H \end{bmatrix} \tag{4.7}$$

Therefore,

$$\Delta V_l = G\,\Delta P_l + H\,\Delta Q_l \tag{4.8}$$

which provides the voltage variation at each load bus l in relation to a load variation at the same bus.

Assume now that the same technique used to determine matrix D_l' is extended to a multi-node system, in the following way:

$$\begin{bmatrix} 0 \\ 0 \\ \Delta\,P_i \\ \Delta\,Q_i \\ \Delta\,P_l \\ \Delta\,Q_l \end{bmatrix} = \begin{bmatrix} A_1 & B_1 \\ C_1 & D_1 \end{bmatrix} \begin{bmatrix} \Delta\,\delta \\ \Delta\,V \\ \Delta\,\delta i \\ \Delta\,V_i \\ \Delta\,\theta_l \\ \Delta\,V_l \end{bmatrix} \tag{4.9}$$

In this case, bus l is the load bus of interest and bus i represents any other load bus. Therefore, C_1 and D_1 define the linear equations of active and reactive power of the buses l and i, respectively. Thus, D_1 has dimension 4×4.

From equation (4.9), it follows that

$$\begin{bmatrix} \Delta P_i \\ \Delta Q_i \\ \Delta P_l \\ \Delta Q_l \end{bmatrix} = \begin{bmatrix} D'_{il} \end{bmatrix} \begin{bmatrix} \Delta \delta i \\ \Delta V_i \\ \Delta \delta_l \\ \Delta V_l \end{bmatrix} \tag{4.10}$$

where D'_{il} contains the partial derivatives of the active and reactive power equations with respect to the variables in the right-hand side vector.

If there are no active and reactive power variations at bus l, then

$$\begin{bmatrix} \Delta P_i \\ \Delta Q_i \end{bmatrix} = \begin{bmatrix} M \end{bmatrix} \begin{bmatrix} \Delta \delta l \\ \Delta V_l \end{bmatrix} \tag{4.11}$$

where M has the same dimension as D'_l. However, instead of relating active and reactive powers of a bus with respect to its voltage magnitude and phase angle, this matrix defines the phase angle and voltage level variation at a load bus in relation to a load variation at another load bus. Hence, the inverse of M provides the variation in voltage magnitude and phase angle at bus l with respect to a load variation at each bus i. A subsystem may then be determined following the steps below:

1. Evaluate equation (3.2) for all load buses.

2. Evaluate equation (4.11) with bus l as the most critical bus.

3. According to a specified tolerance k, find the buses strongly connected to the critical bus. Add levels to the initial critical bus, as described in the foregoing sections, identifying strongly connected buses according to determinant of M

in equation (4.11) and tolerance k. Repeat the process for the most critical of the remaining buses.

This method is computationally robust, because of the large number of operations involved. As an alternative, a second method is proposed, as follows:

1. Evaluate equation (3.2) for all load buses.
2. Sort the vector components obtained in the previous step. Apply Step 3 proposed above to this vector, to obtain the partitioning.

Although this technique is also expensive, it is more efficient than the first alternative proposed in this section since, matrix M of equation (4.11) is not used. This method will be used to obtain the partitioning of a 300 bus system in Chapter 5.

4.5 System Reduction

The system variables that experience small changes during the calculation of the bifurcation manifold by the continuation method are eliminated from the computational process, i.e., a variable x can be fixed at its last equilibrium value if

$$|\Delta x_i| \leq u$$

where u is a specified tolerance [36]. This technique reduces the number of variables and equations used during the continuation process, decreasing consequently the computational burden of tracing bifurcation diagrams.

A problem with this method is the possible elimination of variables associated with system controls with limits, particularly bus voltages with large reactive power

support. These voltages change slowly or do not change at all, until voltage control is lost when minimum or maximum limits are reached. Furthermore, depending on the system variations produced by the parameter λ, an area that initially is not considered critical due to small changes in the associated system variables, could become critical when close to bifurcation. Hence, variables that are eliminated in the early stages of the continuation process, might become later a source of significant computational erros. To minimize this problem one can carry out a system reduction every U number of steps of the continuation process.

Notice that, although this technique eliminates the variables that suffer little change during the voltage collapse process, initially, all the variables are considered, unlike the other techniques proposed so far. Therefore, this technique does not yield a network partition, since no subsystem is calculated.

4.6 Mixed Techniques

The techniques proposed in Sections 4.4.2, 4.4.3 and 4.4.4 provide results based on the initial operating point of a power system. Because of the nonlinearity of power system equations, it is possible that an initial area that is not considered critical becomes critical (or joins the initial critical area) at the bifurcation point. Furthermore, the border buses of a critical area play a very important role on the voltage collapse process, because of the active and reactive powers injection into the critical area, as the system becomes loaded. Therefore, treating border buses as PV buses may lead one to wrong results, specially if generators limits are considered. To overcome this handicap, two alternative methods are proposed:

1. For each subsystem calculated in Sections 4.4.2, 4.4.3 or 4.4.4, calculate the load margin for the whole system, with load changing in each of the subsystems derived from the partitioning techniques. All generators are considered in this case.

2. Use the technique described above with the system reduction technique proposed in Section 4.5. Therefore, besides the consideration of load variation only at a subsystem, the variables that suffer little change during the continuation process are eliminated, reducing even more the computational burden.

   The partitioning techniques proposed here could be applied to general nonlinear systems. This idea of a network partitioning has been exploited for control systems, for example, where the determination of the dominant eigenvalues is required, extrapolating the partitcular example proposed here for a power system.

Chapter 5

TEST RESULTS

5.1 Introduction

This chapter presents the results of the techniques proposed in Chapters 3 and 4. The IEEE 300-bus test system is employed in all simulations. This system has 68 generator buses, 231 load buses, 411 transmission lines and transformers. The tests are carried out in a sun workstation and are divided into two parts, as follows:

1. Voltage collapse indices (eigenvalue and singular values decomposition and test functions) proposed in [38, 43, 51] are evaluated and compared with the reduced load flow Jacobian determinant index, proposed in this thesis. The system is loaded from the initial operating point up to the bifurcation point. For each operating point, the voltage collapse indices are evaluated. The tests are carried out with and without generator limits.

2. Load margin is determined with and without generators limits by a continuation power flow program [25]. This program is briefly described in Appendix

A. To reduce the computational burden, the network partitioning techniques proposed in Chapter 3 are employed.

5.2 Voltage Collapse Indices

In this section, the voltage collapse indices described in Chapter 3 are evaluated and compared.

5.2.1 No Generator Limits

First, the test system is studied with no generator limits. A load increase direction is chosen, according to the initial load at each bus. The system is then driven from an initial operating point up to the bifurcation point by changing the loading coefficient λ, with the help of a continuation power flow [36, 53].

For each operating point, the smallest singular value and smallest absolute eigenvalue are calculated for the load-flow Jacobian J and for the reduced load-flow Jacobian J_{QV}; the results are depicted in Figure 5.1. Observe that the minimum magnitude of the eigenvalues and the minimum singular value of the reduced Jacobian J_{QV}, exhibit "better" behavior than the corresponding values for the full Jacobian J, i.e., they are more sensitive to changes in λ, which agrees with the results and arguments presented in [43]. However, none of these values can be used as an index of proximity to voltage collapse, due to their sharp drop when close to the bifurcation point λ_0.

To study the symmetry of the reduced load-flow Jacobian J_{QV}, its singular values Σ and corresponding eigenvalues Λ are studied. The first observation is that all eigenvalues of J_{QV} are real. Furthermore, these eigenvalues are rather close in

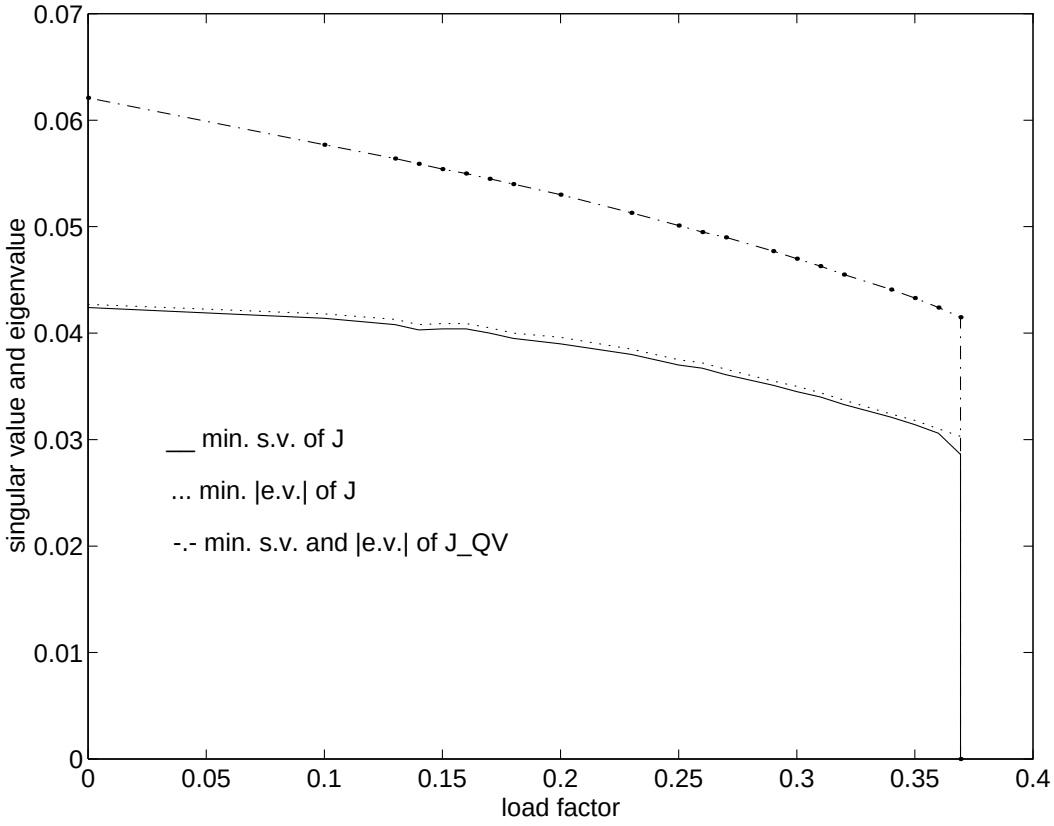

Figure 5.1: Minimum singular value and minimum absolute eigenvalue for the test system with no limits.

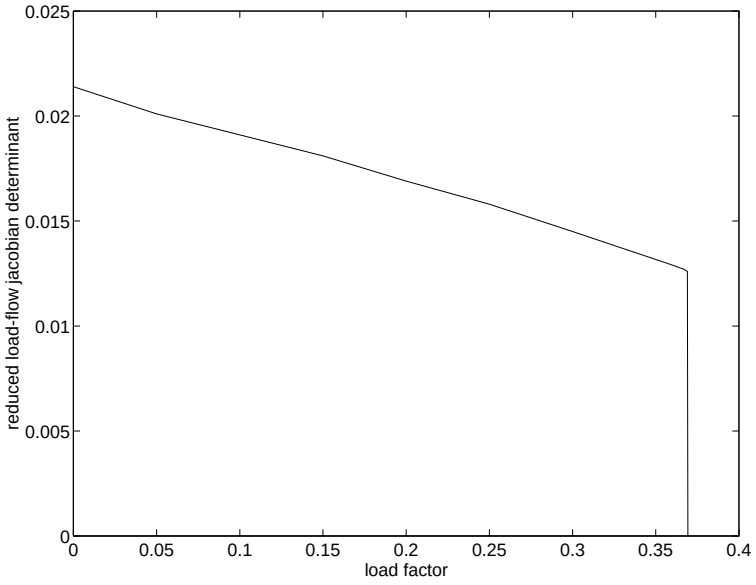

(a)

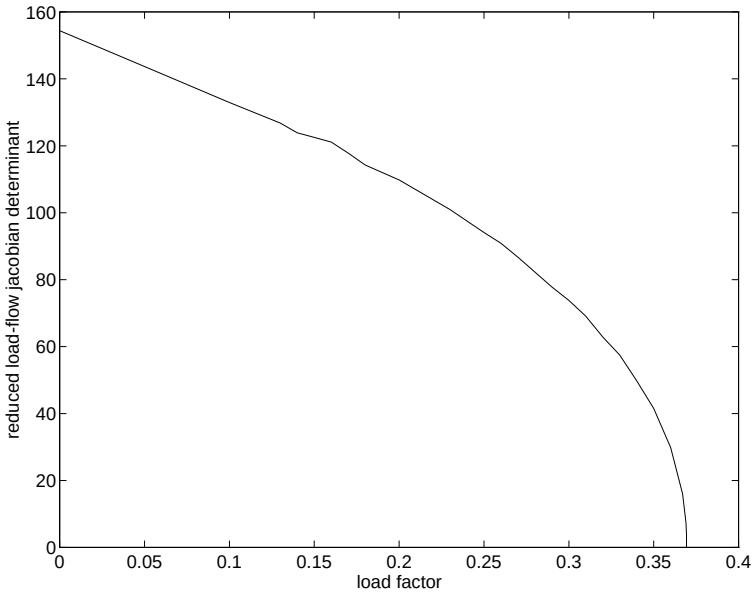

(b)

Figure 5.2: Test function $\det D'_{ll}$ for the test system with no limits evaluated at (a) a non-critical bus $l = 9042$, and at (b) the critical bus $l = c = 192$.

λ_{max}	$\epsilon \times 10^{-5}$
0	1.1792
0.2	1.8465
0.3	2.3538
0.36	2.7038
0.369 (λ_0)	2.7355

Table 5.1: J_{QV} symmetry for system with no limits.

value to the corresponding singular values of this matrix. To illustrate the latter, the following relative error (ϵ) is defined:

$$\epsilon = \frac{||\Sigma - \Lambda||_\infty}{||\Sigma||_\infty} \tag{5.1}$$

or

$$\epsilon = \frac{max_i\,(\sigma_i - \mu_i)}{max_i\,(\sigma_i)} \tag{5.2}$$

This error is evaluated for several operating points, up to the critical or maximum loading coefficient λ_0. The results of these computations for the system without limits are shown in Table 5.1. The value of ϵ increases slightly as the minimum singular value and absolute eigenvalue approach zero. However, overall this value remains rather small, indicating that both singular value and eigenvalue decomposition are basically the same.

Figure 5.2 illustrates the shape of the test function det D'_{ll} for the actual critical bus ($c = 192$) and for a bus judged as critical at the initial operating point ($l = 9042$). Notice the striking similarity of the general shapes of this test function to

the ones depicted in Figure 5.3, for $|t_{ll}|$. In both cases, only the test functions evaluated at the critical bus have the quartic shape required by the performance index τ, defined in Section 3.4.4. Bus 9042 is associated to the largest entry of the tangent vector at the initial operating point, therefore, it is the initial critical bus. This is confirmed by the smallest reduced Jacobian determinant. However, bus 192 becomes critical when the system is operating very close to the voltage collapse point. In this case, the actual critical bus cannot be determined from the tangent vector information at operating points away from the bifurcation. Reference [34], however, shows that for the IEEE 24-bus system, the initial critical bus and area are the same as the critical at the bifurcation point. That particular result has also been found for the IEEE 30-bus system in [37]. The results obtained in this section, however, show that those results can not be extrapolated for larger power systems.

The PV curves, nose curves, or bifurcation diagrams of the test system without limits are shown in Figure 5.4, to depict the voltage behavior for the buses under study.

5.2.2 With Generators Limits

The test system with all limits considered is employed here to show several of the shortcomings of the indices and test functions, which are not addressed in [43] and [51].

The minimum singular values and absolute eigenvalues of J and J_{QV} are again monitored for changes in λ, as depicted in Figure 5.5. Similar results to those obtained in the previous case are observed, i.e., the indices show a sudden large drop when close to the bifurcation point, rendering them inadequate for detecting proximity to a collapse point. The singular values and eigenvalues of J_{QV} are analyzed

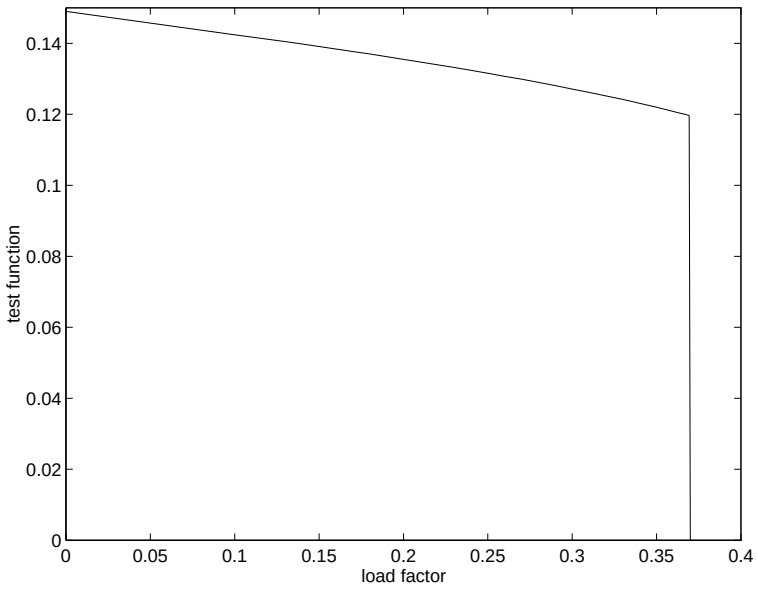

(a)

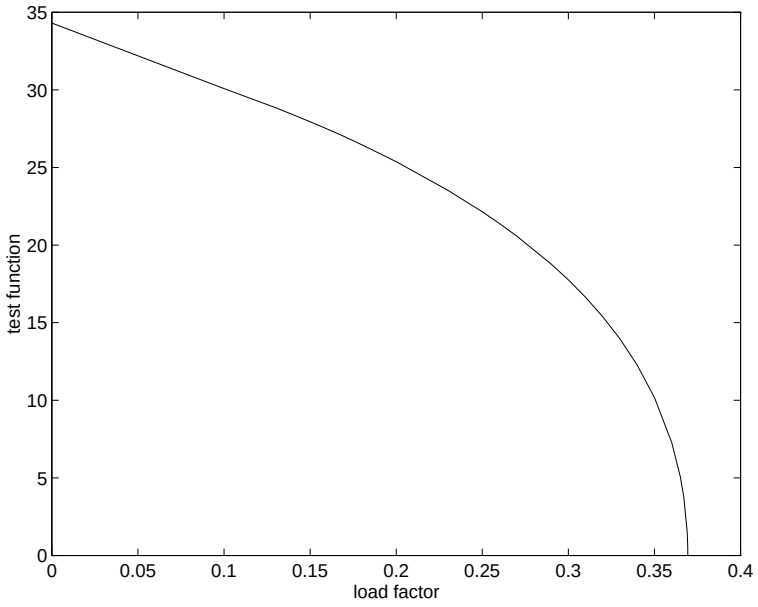

(b)

Figure 5.3: Absolute value of the test function t_{ll} for the test system with no limits evaluated at (a) a non-critical bus $l = 9042$, and at (b) the critical bus $l = c = 192$.

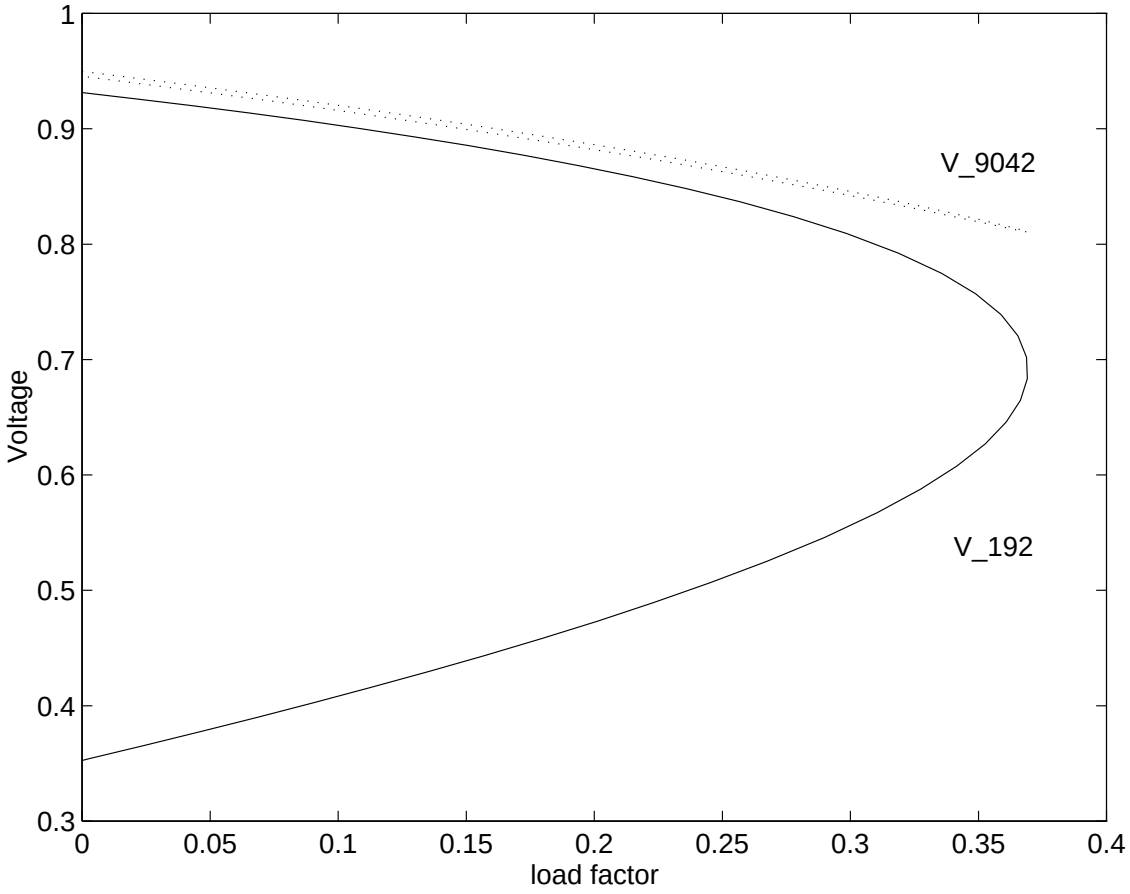

Figure 5.4: PV curve or bifurcation diagram for the test system without limits.

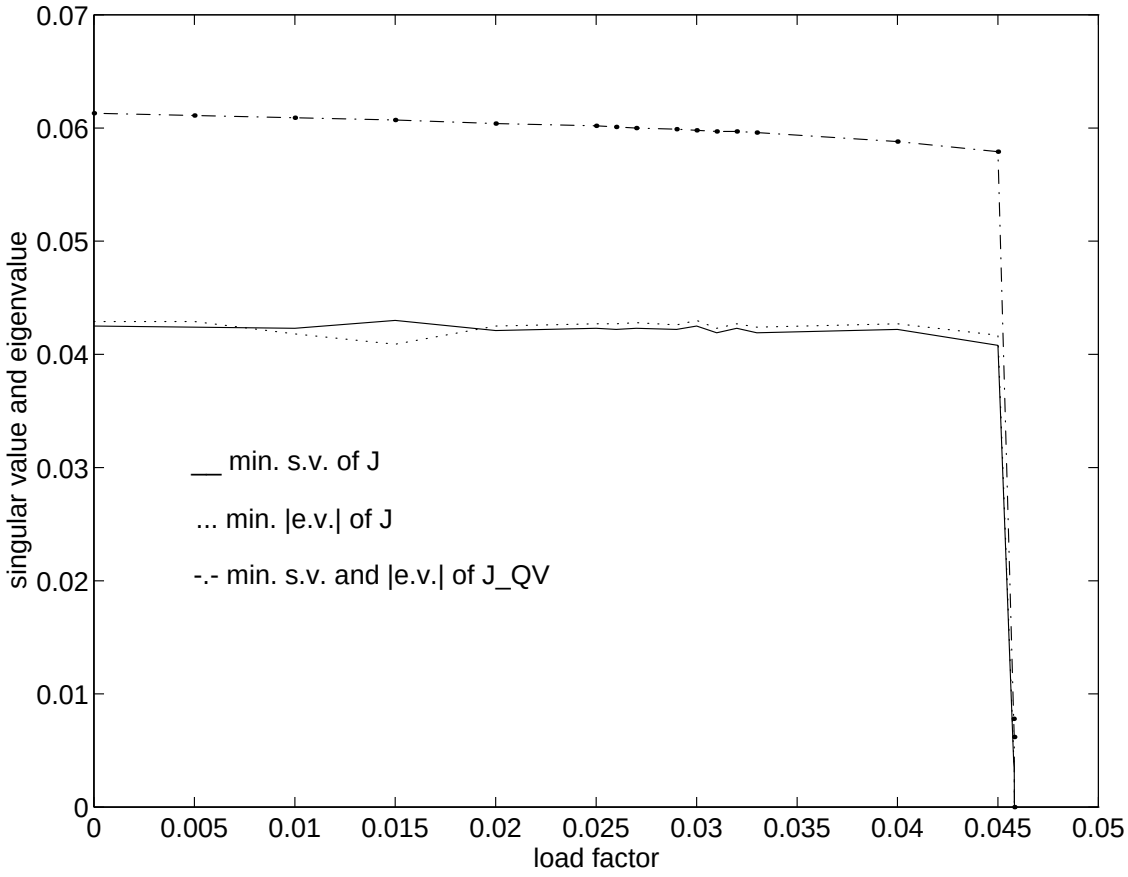

Figure 5.5: Minimum singular value and minimum absolute eigenvalue for the test system with limits.

for symmetry, with similar results to those obtained with no limits consideration.

Figures 5.6 and 5.7 show the test functions $\det D'_{ll}$ and $|t_{ll}|$, respectively, for two distinct system buses. Bus 192 corresponds to the system critical bus when no limits are considered, whereas bus 526 is the actual critical bus of the system when the limits are applied. First, notice the similarity once again between the test functions. Second, the critical bus test function does not present a quartic or quadratic shape as required for the computation of τ. However, it is better

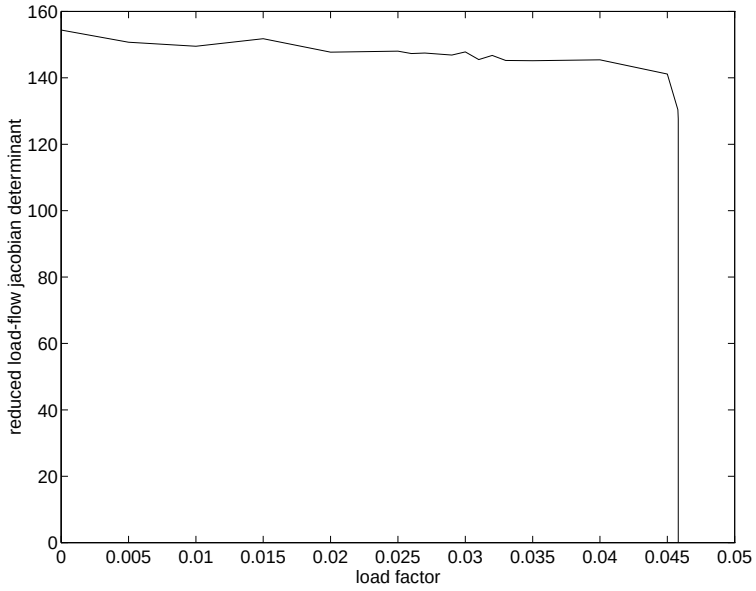

(a)

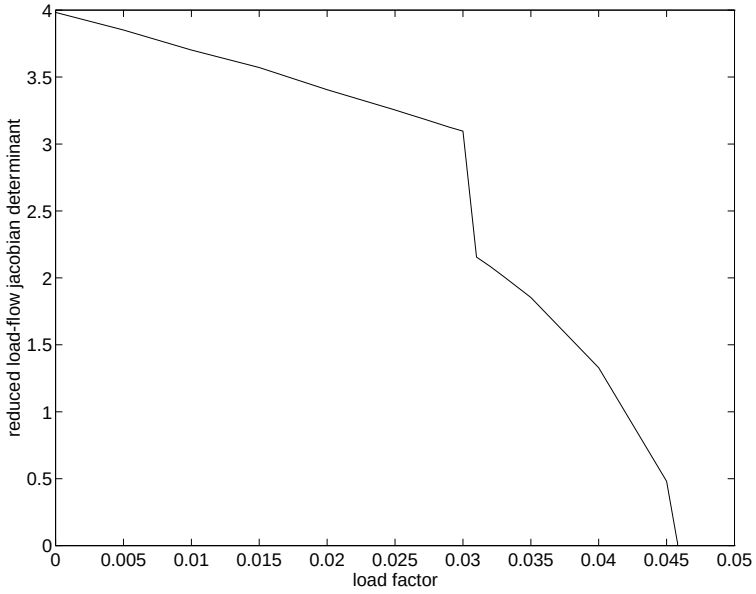

(b)

Figure 5.6: Test function $\det D'_{ll}$ for the IEEE 300 bus test system evaluated at (a) a non-critical bus $l = 192$, and at (b) the critical bus $l = c = 526$.

behaved than the test function of a bus other than the critical one. In this case, the performance index τ is not well defined due to the discontinuity in $\det D'_{cc}$ and t_{cc}, depicted in Figures 5.6 and 5.7. On the other hand, the results are better than those presented by singular values and eigenvalues of J and J_{QV} shown in Figure 5.5. Once more, the critical bus can only be detected when the system is very close to the bifurcation point. Notice , however, that if the initial operating point is assumed as the one defined by $\lambda = 0.035$ in Figure 5.6, a smooth behavior of the reduced Jacobian determinant is obtained. This result would lead one to conclude that the quadratic behavior obtained without limits consideration would also be present here. Therefore, voltage collapse point determination depends not only on the system under analysis, but also on its operating point.

Figure 5.8 depicts the PV curves of the test system with limits considered to illustrate the voltage behavior for the buses under study. Notice, in this case, the little change in bus voltage magnitude at bus 192 compared with the changes shown in Figure 5.4.

The results discussed above show that critical bus and area determination play a very important role on voltage collapse analysis. Reference [48] assumes that the initial system critical bus and area remain the same during the voltage collapse process. This consideration arises from the assumption that the singular vectors do not change significantly when far from the bifurcation point. References [35, 36, 50], however, show that this assumption is not necessarily true in all power systems, as demonstrated here for the IEEE 300-bus system. In Table 5.2, one observes that the right eigenvector entries change significantly as the system is loaded. Furthermore, the changes are highly nonlinear, as one can see for the actual critical bus rank position. These changes depend on the load increase direction, i.e., for a different loading direction, the corresponding eigenvectors change in other ways.

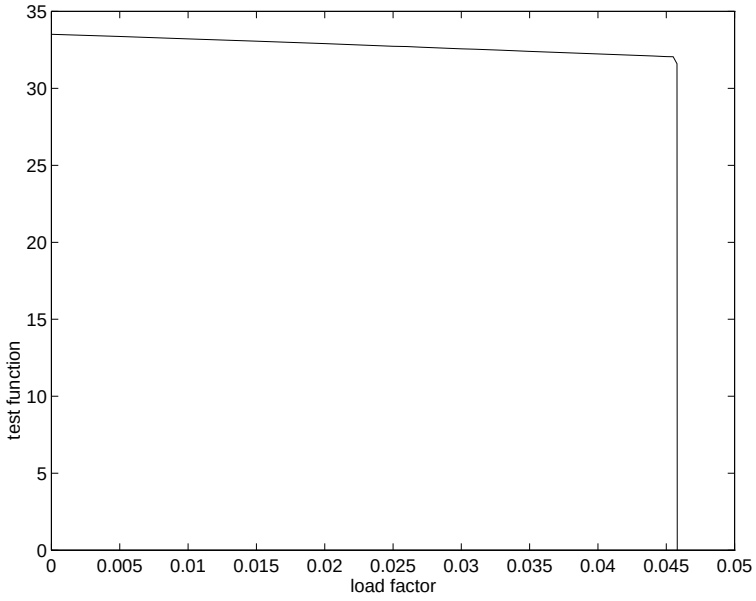

(a)

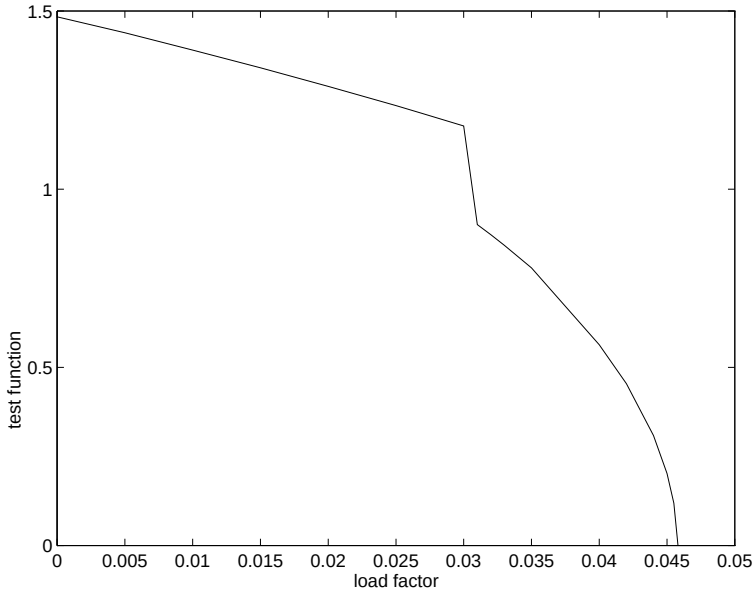

(b)

Figure 5.7: Absolute value of the test function t_{ll} for the IEEE 300 bus test system evaluated at (a) a non-critical bus $l = 192$, and at (b) the critical bus $l = c = 526$.

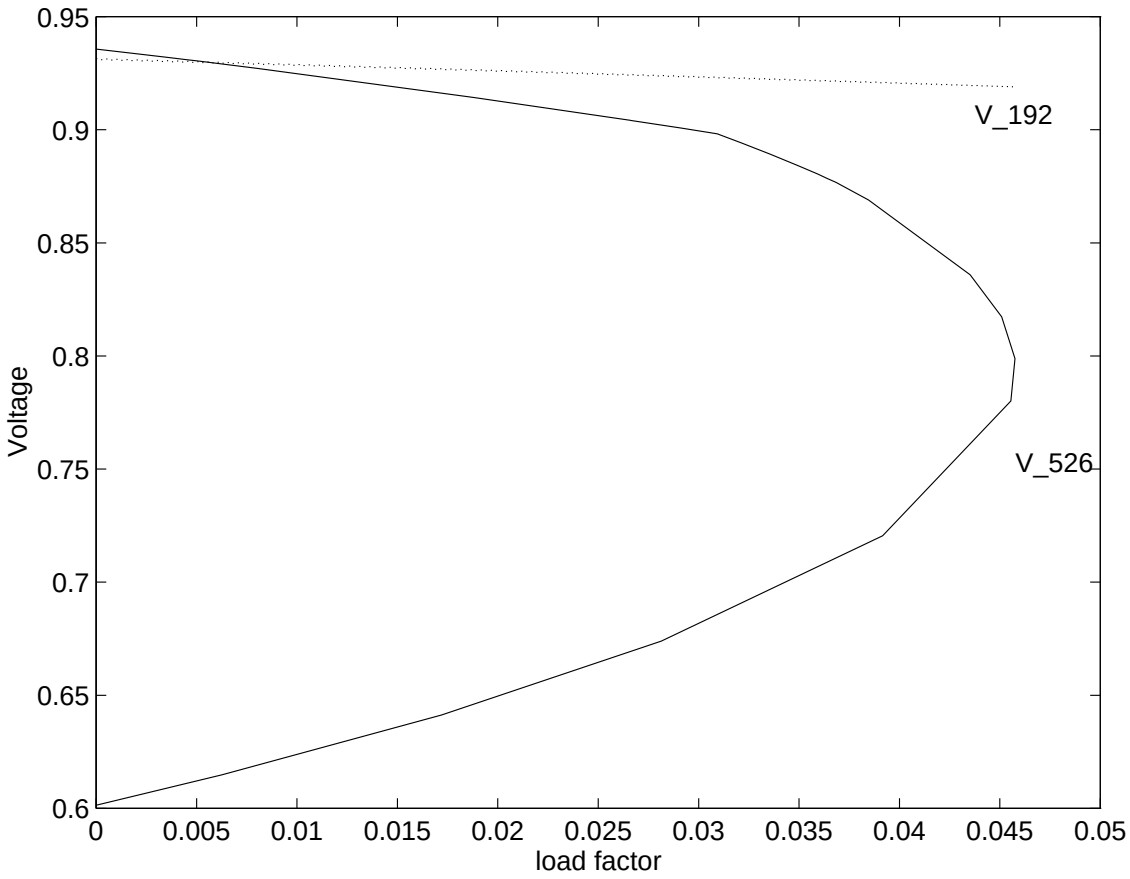

Figure 5.8: PV curve or bifurcation diagram for the test system with limits.

λ_{max}	*Critical Bus*	*Bus 192 Rank*	v_{9042}	v_{192}
0	9042	74	1.000	0.0125
0.12	9042	74	1.000	0.0154
0.24	9033	75	0.965	0.0172
0.36	9033	76	0.912	0.0187
0.365	9033	75	0.908	0.0192
0.369	9033	71	0.759	0.0194
0.3693	9033	36	0.210	0.0189
0.36933	9033	19	0.088	0.0178
0.36934	192	1	0.0004	0.0185

Table 5.2: 300 bus system critical buses.

The results of Table 5.2 brings out a very important and still open question in voltage collapse analysis, regarding the critical bus determination. Because of the sharp critical bus rank variation at the bifurcation point, it is not possible to predict which bus will become the critical one at the bifurcation. A technique to calculate the critical bus a priori must be studied further.

5.3 System Partitioning and Reduction

5.3.1 General Aspects

This section employs network partitioning and system reduction techniques to reduce the computational burden of continuation methods.

Load margin determination is carried out for:

Case	λ_{max} *Continuation Method*	λ_{max} *Direct Method*	*Critical Bus*
With Limits	0.04575	0.04576	526
No Limits	0.36908	0.36934	192

Table 5.3: Load margin for the IEEE 300 bus system.

1. Whole system, with no approximations or reductions.
2. Subsystems found by right eigenvector, tangent vector and reduced Jacobian determinant techniques.
3. Whole system with load variation at each subsystem calculated by the same partitioning techniques of item 2.
4. Whole system using system reduction technique.
5. Whole system using mixed technique.

The estimated load margin obtained in items 2 to 5 is compared with the load margin calculated for the whole system in item 1.

5.3.2 Load Margin for the Whole System

The load margins obtained here by the direct method will be compared with those obtained in other sections. Table 5.3 shows the results with and without generators limits, for continuation and direct methods.

System	*Time (s)*	λ_{max}	*Error (%)*	*PQ buses*
Subsystem 1	5.1	1.25	+238.44	41
Subsystem 2	22.5	0.63746	+72.59	167

Table 5.4: Load margin for the subsystems. No limits.

5.3.3 Network Partitioning by Right Eigenvector

The results of applying the technique proposed in Section 4.4.2 are presented here. References [18, 34, 36] show that the critical area of a power system is not strongly affected by load changes in the remaining buses. Based on that, an area obtained from the initial critical bus can be determined, and voltage collapse analysis carried out for this reduced system. The remaining critical buses are used to obtain other subsystems. Each subsystem is considered as an isolated power system; the subsystem with the smallest load margin is considered the critical one. The critical bus of this subsystem is evaluated at the bifurcation point and compared with the critical bus for the whole system. The error shown in all tables is defined as

$$Error = \frac{\lambda_{sub} - \lambda_{whole}}{\lambda_{whole}}$$

where λ_{sub} is maximum load margin for the subsystems, and λ_{whole} is the maximum load margin for the whole system.

This technique has been implemented in MATLAB [63], and the results are shown in Table 5.4, for the test system with no limits. The tolerance value k defined in Section 4.4.2 is chosen as 0.75, for which the technique provides a two-block partitioning. The critical bus at the bifurcation point for the critical subsystem (Subsystem 2) is 192, the same as that for the whole system.

The large errors observed in Table 5.4 clearly show that this technique is not adequate. This is due to problems with defining the active and reactive-power injections at the critical area during the voltage collapse process. These powers cannot be predicted by considering the neighboring buses as PV buses. Better results are obtained by only considering the subsystem as the system area where load variation occurs, and the rest of the system remains unchanged. Notice that this assumption keeps all system generators, avoiding the error introduced by assuming the neighboring buses as PV buses.

5.3.4 Area Load Increase

This section presents the results when the subsystems are not treated independently, but considered as the only areas where load is allowed to change.

Right Eigenvector Technique

As shown in Section 5.3.3, for $k = 0.75$ the technique provides a two-block partitioning. Table 5.5 shows the result for each subsystem load increase. Subsystem 1 is the initial critical area of the system, whereas Subsystem 2 contains the actual critical bus at the bifurcation. Notice that the critical area may be reduced further as the system is loaded. Also, notice that the large error obtained when limits are considered indicates that the absence of load variation in the remaining buses influence the results.

The computational time per step when load is increased at area 2 is 1.464 seconds without generators limits, and 1.47 seconds when generators limits are considered. This C.P.U. time can be improved using better factorization routines in PFLOW. On the other hand, the partitioning technique must be improved, since

	No limits			*With limits*			
System	*Time* (s)	λ_{max}	*Error* (%)	*Time* (s)	λ_{max}	*Error* (%)	*Number of PQ buses*
Subsystem 1	39.5	0.58733	+59.02	96.3	0.17824	+290	42
Subsystem 2	45.9	0.36414	+1.4	51.1	0.0567	+23.9	167

Table 5.5: Load margin for subsystems load increase. Right eigenvector technique.

in that case, after obtaining the first block partitioning, the remaining buses have been considered as the other block partitioning. These observations are valid for all partitioning techniques presented in this section.

Figure 5.9 shows the PV curve of bus 192 (critical bus) when generators limits are not considered, and Figure 5.10 shows the PV curve of bus 526 (critical bus) when generators limits are considered. The solid line represents the base case of Section 5.3.2, and the dashed line represents the voltage variation for the subsystem with the critical bus; the same applies for all figures shown in this section.

It is important to stress that Subsystem 2 (the critical one) does not contain the initial critical bus of the system, as already mentioned in Section 5.2.1. This result shows that it is not possible, for a known operating point, to predict which area of the system will be the critical at the bifurcation. In [34], the initial critical area remains the same during the continuation process for the IEEE 24-bus system, and hence better partitions are obtained.

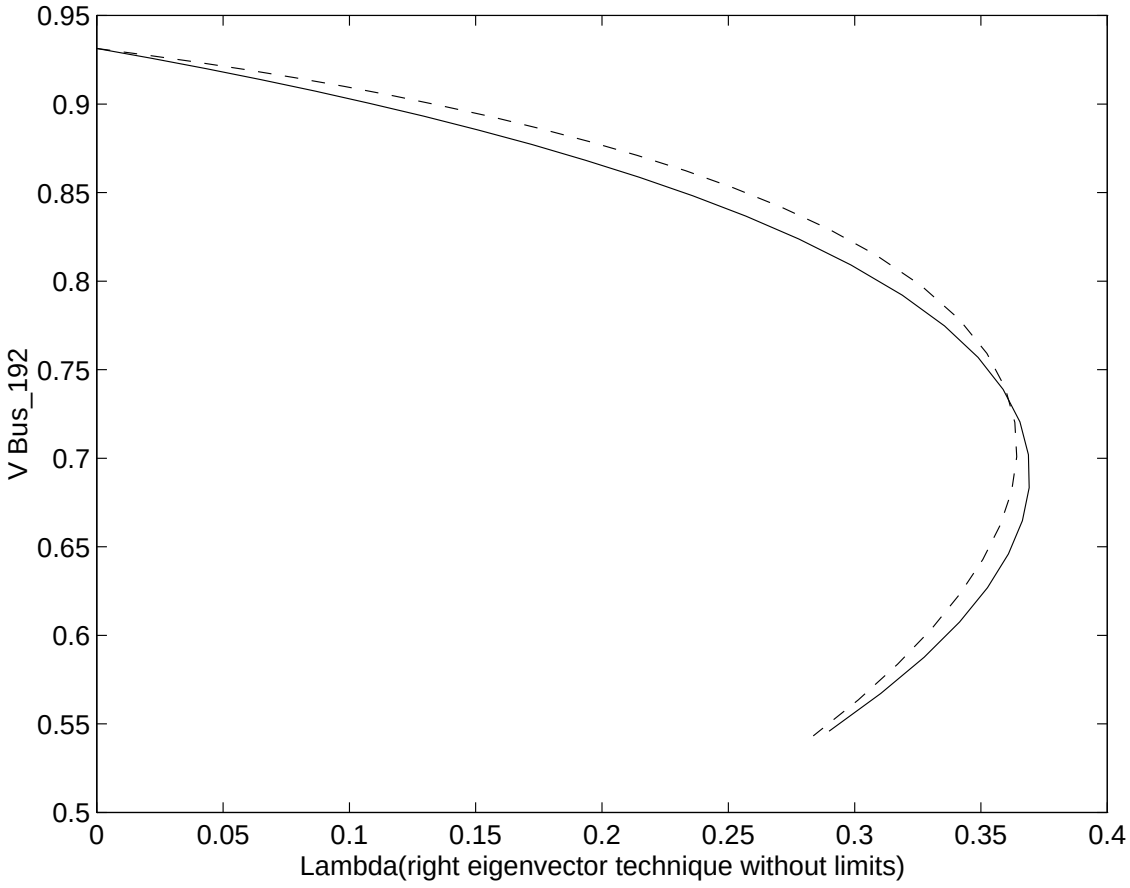

Figure 5.9: Bifurcation diagrams (PV or nose curves) of bus 192 when the right eigenvector technique is applied and no limits are considered.

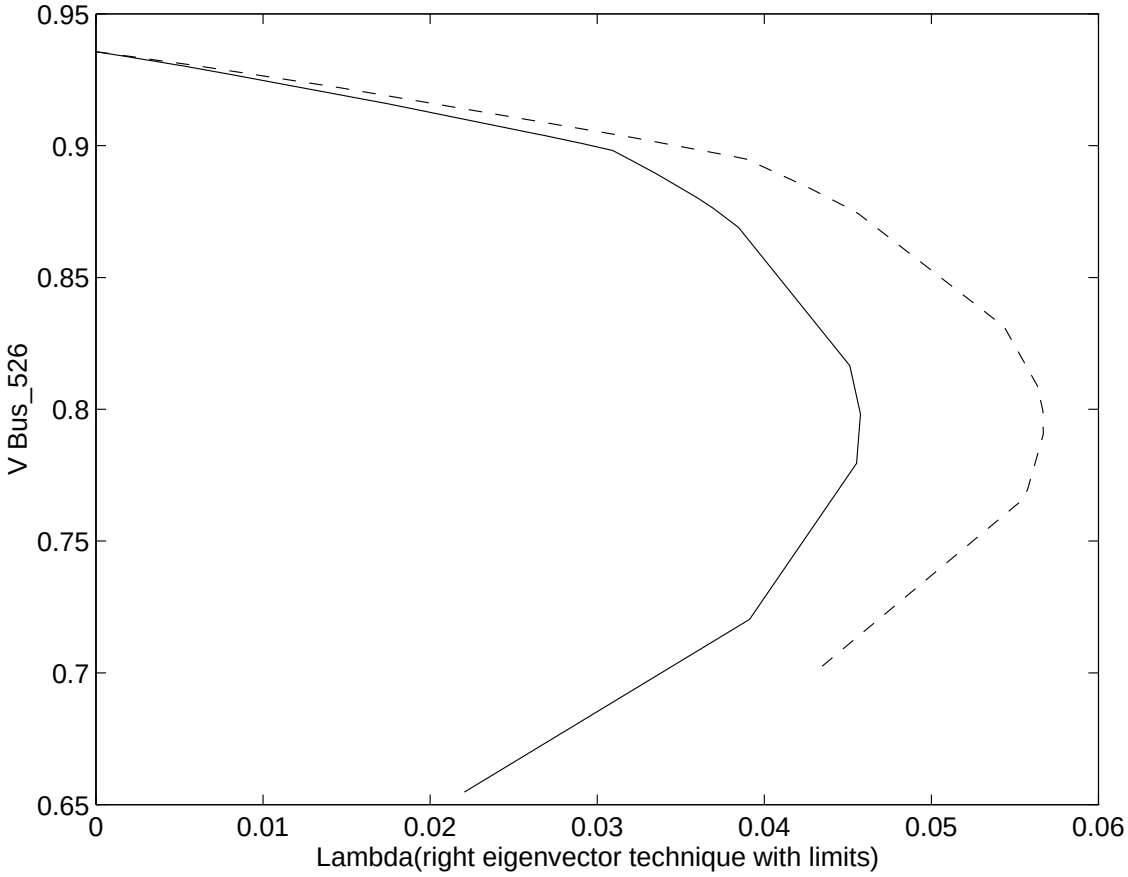

Figure 5.10: Bifurcation diagrams (PV or nose curves) of bus 526 when the right eigenvector technique is applied and limits are considered.

	No limits			*With limits*			
System	*Time* (s)	λ_{max}	*Error* (%)	*Time* (s)	λ_{max}	*Error* (%)	*Number of PQ buses*
Subsystem 1	39.2	0.58802	+59.32	96.3	0.17824	+190	42
Subsystem 2	60.4	0.30448	-17.5	77.8	0.06565	+43.65	94
Subsystem 3	47.3	0.66726	+80.79	71.7	0.21487	+370	25

Table 5.6: Load margin for subsystems load increase. Reduced determinant technique.

Reduced Jacobian Determinant Technique

Table 5.6 shows the results of the three-block partitioning obtained for $k = 0.8$, when the reduced Jacobian determinant technique is used.

Figure 5.11 shows an almost invariant voltage at bus 192 with respect to load increase at Subsystem 2, the system with the smallest λ_o. This is due to bus 192 having no load variation during the voltage collapse process, as the technique eliminates the critical bus from the loading areas. When limits are considered, the critical bus is correctly included in Subsystem 2, but a large error is still observed, since only 94 PQ buses have load variation during the voltage collapse process. The computational time per step for Subsystem 2 is 2.23 seconds without generator limits, and 1.44 seconds when generator limits are considered. Figures 5.12 shows the PV curve of bus 526, when limits are considered.

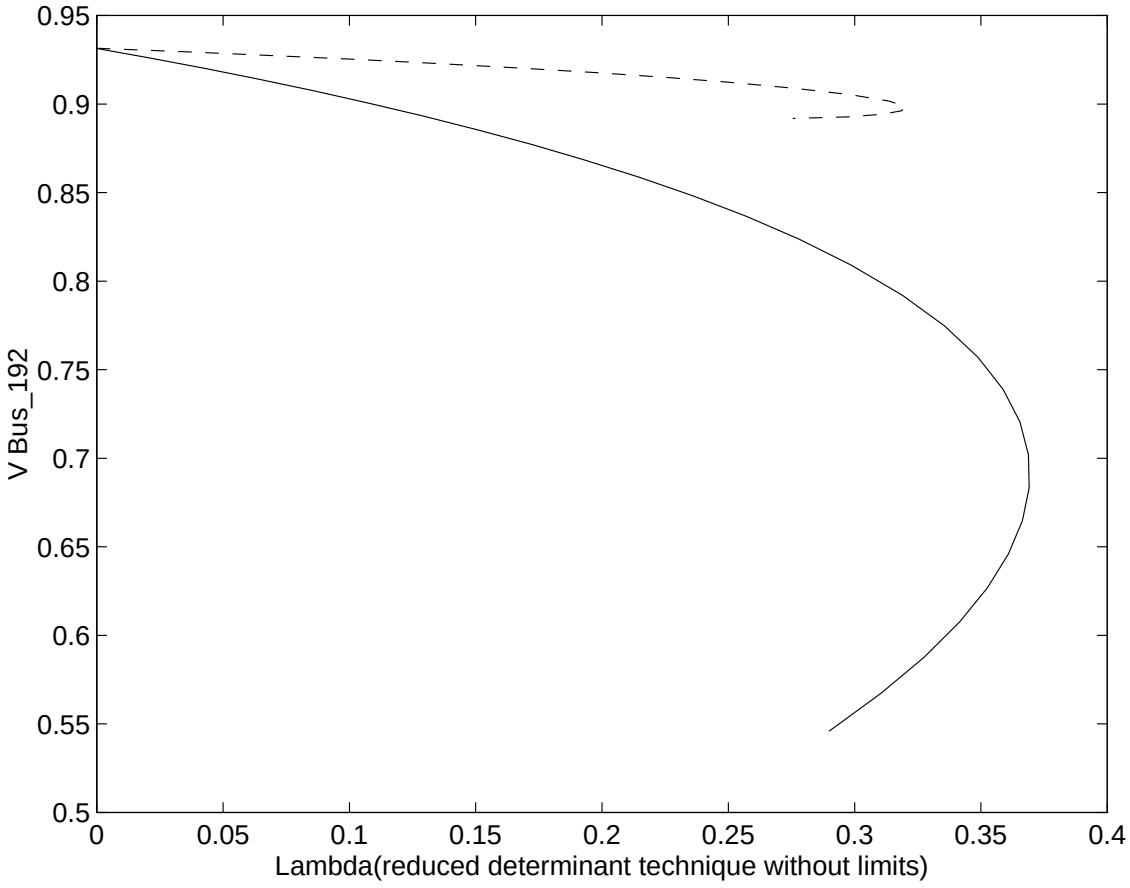

Figure 5.11: Bifurcation diagrams (PV or nose curves) of bus 192 when the reduced Jacobian determinant technique is applied and no limits are considered.

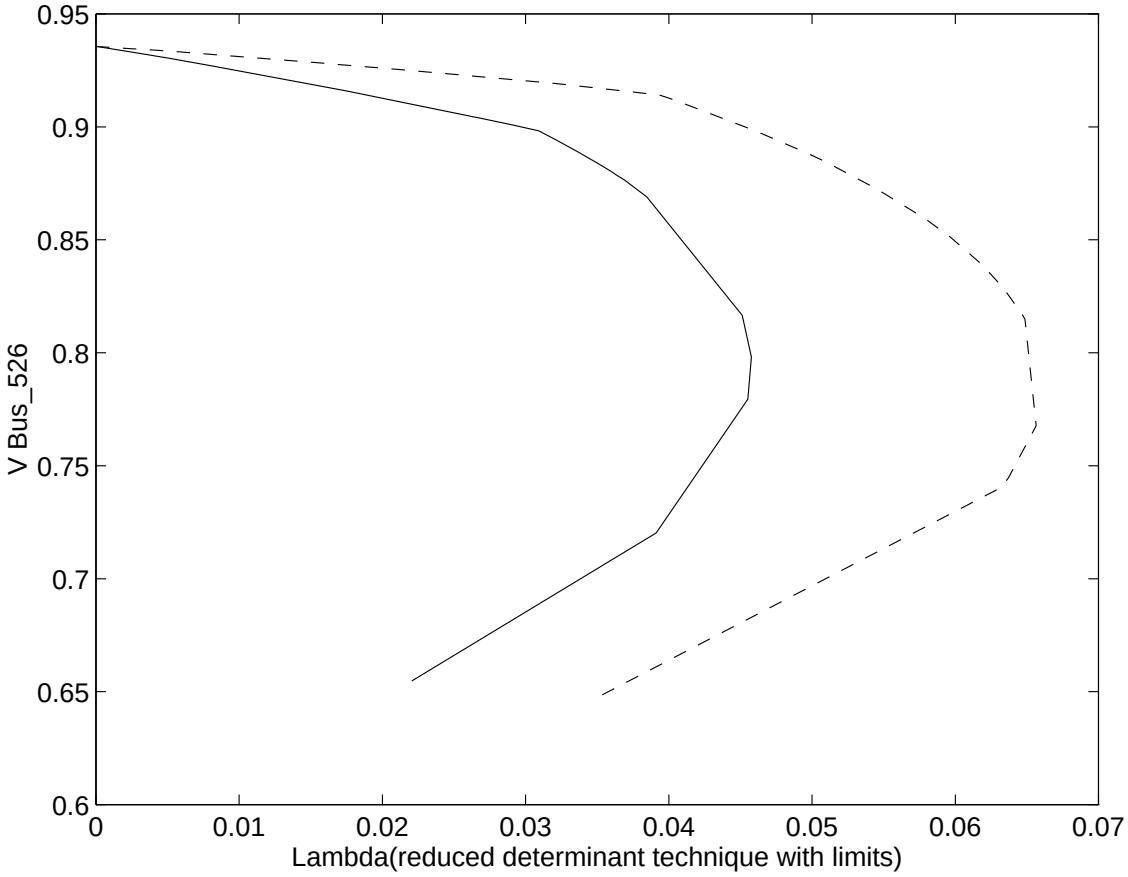

Figure 5.12: Bifurcation diagrams (PV or nose curves) of bus 526 when the reduced Jacobian determinant technique is applied and limits are considered.

	No limits			*With limits*			
System	*Time* (s)	λ_{max}	*Error* (%)	*Time* (s)	λ_{max}	*Error* (%)	*Number of PQ buses*
Subsystem 1	45	1.6817	+356	116.3	0.9172	+1904	15
Subsystem 2	42.4	0.37067	+4.3	76	0.0467	+2.05	226

Table 5.7: Load margin for subsystems load increase. Tangent vector technique.

Tangent Vector Technique

Since the tangent vector provides the voltage and phase angle variations with respect to load increase λ, it will be used here to determine the areas where load should be increased. The main advantage of this method is the low computational time required. Unlike right eigenvector and reduced Jacobian determinant techniques, the tangent vector is obtained in one step. Table 5.7 shows the results of this technique for $k = 0.5$.

Comparing the results obtained by the tangent vector technique shown in Table 5.7 with those shown in Tables 5.5 and 5.6, one can see that a larger initial critical area is calculated, and better results are obtained when generator limits are considered. The results indicate that although the actual critical area is reduced as the system approaches the bifurcation, the elimination of too many buses from the very beginning of the continuation process produce inaccurate results. The actual critical buses are the same as those identified in Section 5.3.2. The computational time per step of Subsystem 2 is 1.5 without generator limits, and 1.47 when generator limits are considered. Figures 5.13 and 5.14 show the results when generator limits are neglected and considered, respectively; again, the solid line corresponds to the base case and the dashed line corresponds to Subsystem 2. Notice that the

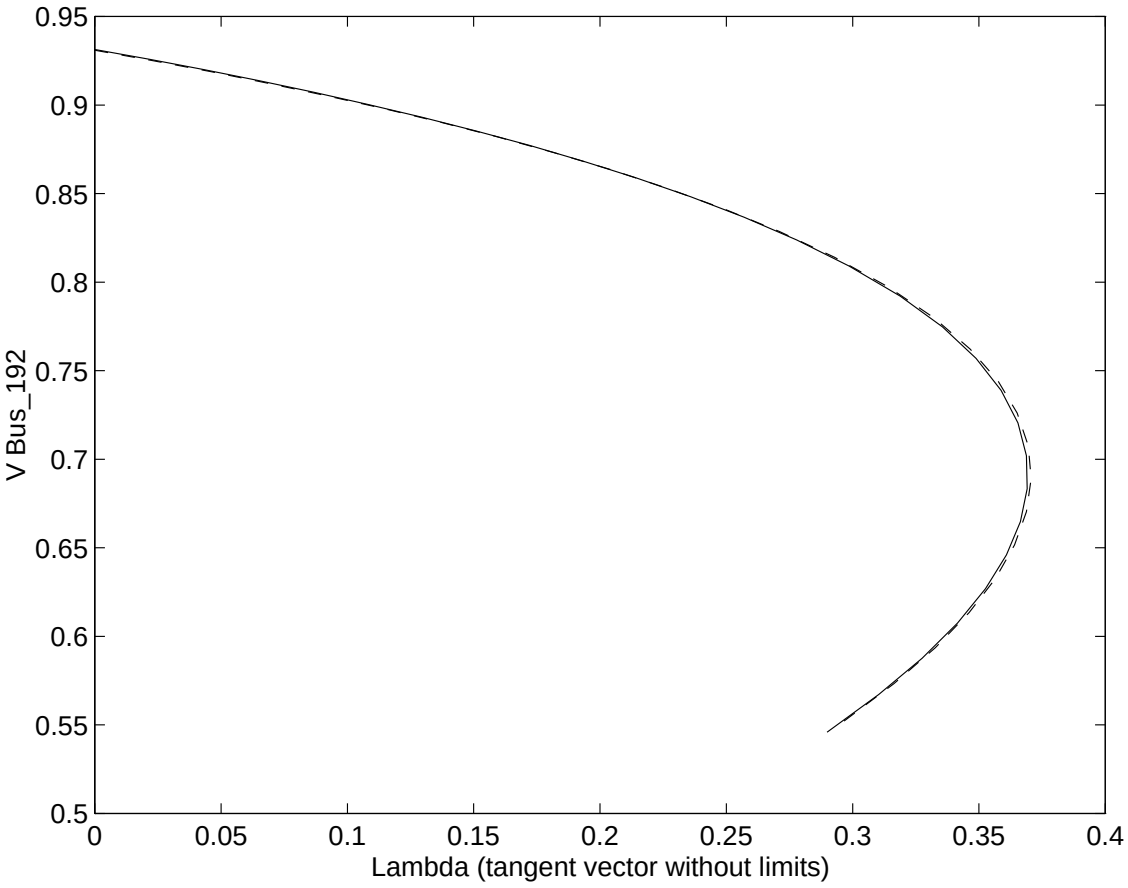

Figure 5.13: Bifurcation diagrams (PV or nose curves) of bus 192 when the tangent vector is applied and no limits considered.

very small errors indicate that this technique may provide good results, but the computational time may be improved by further investigation.

5.3.5 System Reduction

The tangent vector reduction technique has been incorporated into PFLOW [25], which was used to obtain the results of this section.

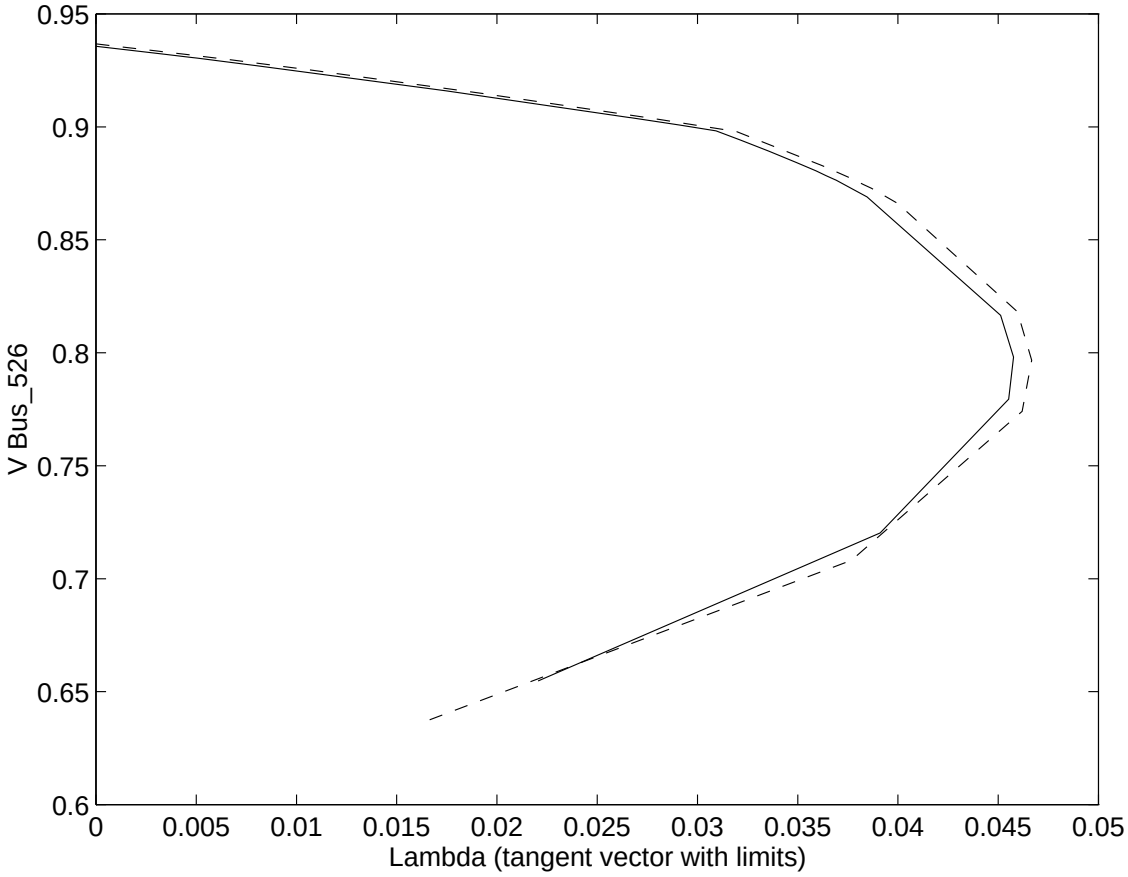

Figure 5.14: Bifurcation diagrams (PV or nose curves) of bus 526 when the tangent vector technique is applied and limits considered.

Case No.	*Reduction Data*	*Number of Equations*	*Time* [s]	*Time/step* [s]	λ_{max}	*Error* [%]
1	$u = 0$ $U = \infty$	600	43.2	1.4897	0.36908	-0.07
2	$u = 10^{-6}$ $U = 2$	596	46.7	1.6103	0.36908	-0.07
3	$u = 10^{-4}$ $U = 2$	460	46.2	1.5931	0.36908	-0.07
4	$u = 10^{-3}$ $U = 10$	407	46.5	1.6034	0.37337	+1.09
5	$u = 10^{-3}$ $U = 5$	395	51.6	1.7793	0.37598	+1.80
6	$u = 10^{-3}$ $U = 2$	64	67.1	1.7205	0.37968	+2.80

Table 5.8: Results of the tangent vector reduction technique with no limits considered.

Table 5.8 and Figure 5.15 show the results obtained for increasing load throughout the whole system when no limits are considered, whereas Table 5.9 and Figure 5.16 show the results for increasing load throughout the whole system when generators limits are considered. These tables are obtained considering several values of tolerance u to be applied each U steps. For each pair of u and U, the total computational time and time per step are depicted. The error in the results is also given. The number of load flow equations at the collapse point is also illustrated with respect to the actual value of λ_o.

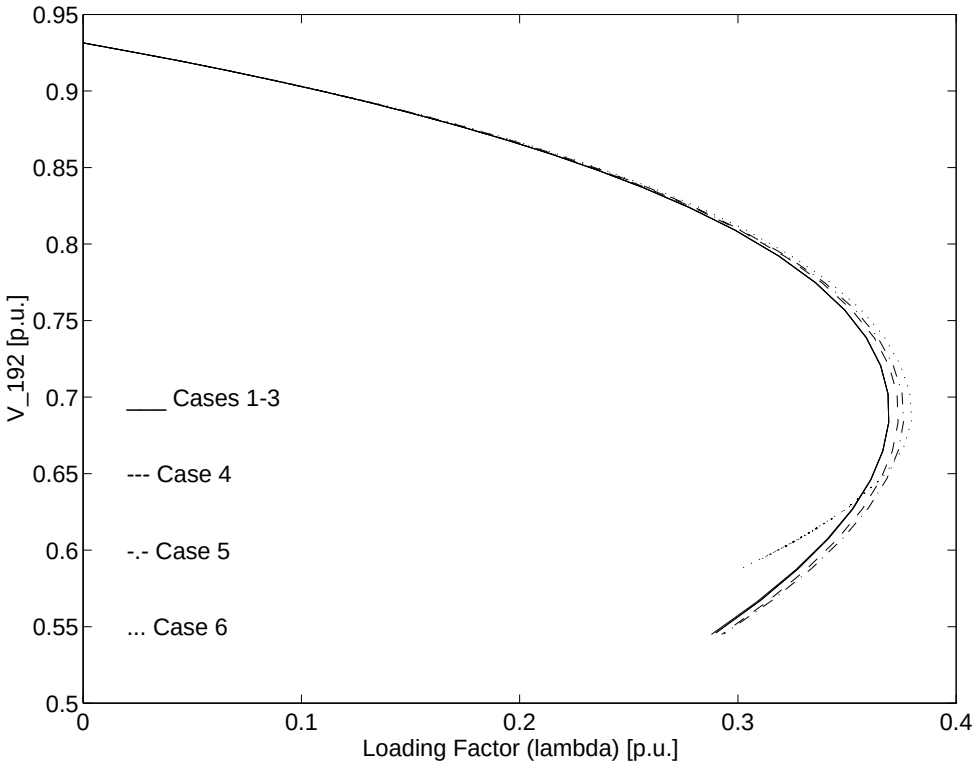

Figure 5.15: Bifurcation diagrams (PV or nose curves) for bus 192 voltage for the original and reduced systems when *no limits* are considered.

Case No.	*Reduction Data*	*Number of Equations*	*Time* [s]	*Time/step* [s]	λ_{max}	*Error* [%]
7	$u = 0$ $U = \infty$	600	75.6	1.3263	0.04575	-0.03
8	$u = 10^{-6}$ $U = 2$	598	76.9	1.3491	0.04575	-0.03
9	$u = 10^{-4}$ $U = 2$	582	82.0	1.4386	0.04563	-0.29
10	$u = 10^{-3}$ $U = 10$	513	87.1	0.9678	0.04927	+7.67
11	$u = 10^{-3}$ $U = 5$	446	114.6	1.6141	0.04943	+8.01
12	$u = 10^{-3}$ $U = 2$	450	104.4	1.5353	0.04953	+8.23

Table 5.9: Results of the tangent vector reduction technique with limits considered.

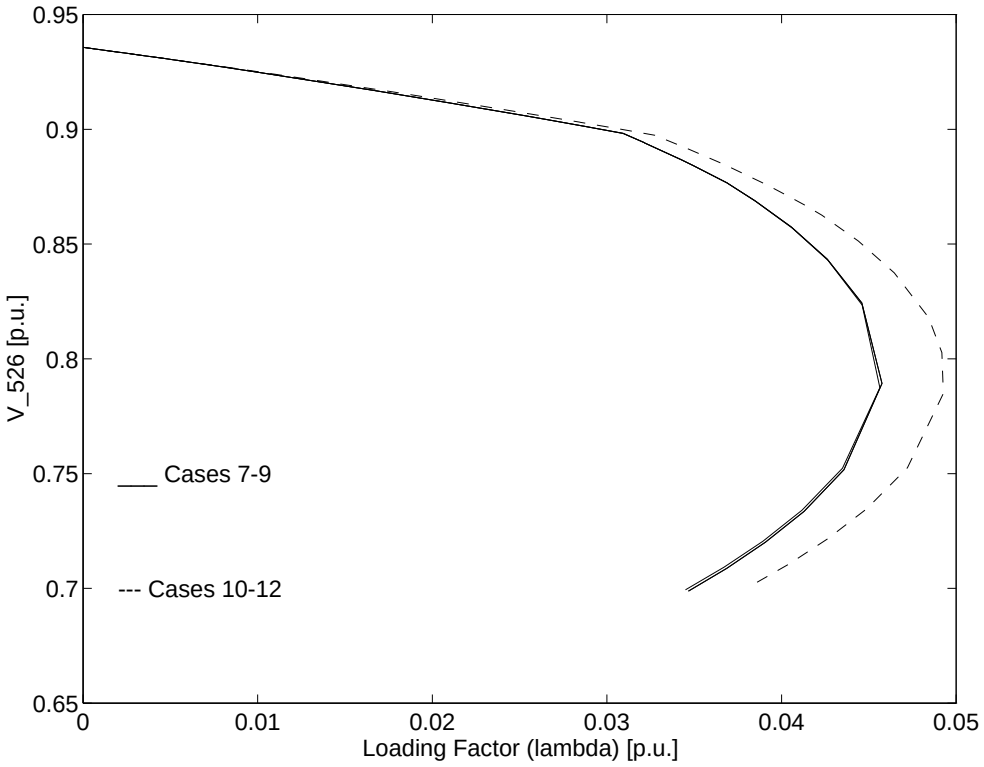

Figure 5.16: Bifurcation diagrams (PV or nose curves) for bus 526 voltage for the original and reduced systems when *limits* are considered.

From these results one can conclude, in general, that the smaller the values of u and U, the smaller the number of equations used and, therefore, the larger the errors are. Also, as the criterion tolerance u and the number of steps U decreases, the CPU time per step of the continuation method tends to decrease, as expected. Notice that in some cases the CPU time tends to increase even though the number of equations decreases. This is due to the requirement of a refactorization of the Jacobian matrix when the number of equations changes; thus, the smaller the value of U, the more often this has to be done along the bifurcation manifold, and consequently, the larger is the CPU time.

5.3.6 Network Partitioning and System Reduction

This section presents the results of the mixed system reduction technique described in Section 4.6.

Right Eigenvector Partitioning and System Reduction Techniques

Table 5.10 shows the results when right eigenvector partitioning is mixed with the system reduction technique, and no generators limits are considered. Small errors are observed, but the computational time per step is larger than the one obtained by the right eigenvector technique alone (Section 5.3.4). This computational time may be reduced if the PFLOW program improves the factorization process, and this observation is valid for all the other mixed techniques tested in this section. In this table one can see that reducing the number of equations does not increase the error significantly, providing good results.

Table 5.11 shows the results when generators limits are considered. This table shows that the error initially observed in Section 5.3.3 increases when the system

u	U	*Comp. Time (s)*	*Comp. Time/Step*	λ_{max}	*Error (%)*	*Number of Equations*
10^{-3}	4	44.6	1.538	0.3867	+4.7	348

Table 5.10: Load margin for system reduction and right eigenvector. No limits.

u	U	*Comp. Time (s)*	*Comp. Time/Step*	λ_{max}	*Error (%)*	*Number of Equations*
10^{-3}	10	58.7	1.82	0.0660	+44.4	373

Table 5.11: Load margin for system reduction and right eigenvector. With limits.

reduction technique is applied. This is expected, since several load buses have fixed loads from the beginning of the process, and consequently, the variables associated to these buses may change only slightly and are eliminated when the system load changes.

Tangent Vector Partitioning and System Reduction Techniques

Table 5.12 shows the results of system reduction mixed with the tangent vector partitioning technique, when no generators limits are considered. The small error observed indicates that the reduced number of equations still provides good results, although the computational time must be improved.

Table 5.13 shows the results when generators limits are considered. These results are close to those obtained in Section 5.3.2. Notice that the number of equations is larger than the number of equations shown in Table 5.12. This is because the reactive power distribution changes when generators limits are considered, affecting bus voltages that do not change significantly when these limits are neglected.

u	U	*Comp. Time (s)*	*Comp. Time/Step*	λ_{max}	*Error (%)*	*Number of Equations*
10^{-3}	10	44.9	1.548	0.37322	1.12	376

Table 5.12: Load margin for system reduction and tangent vector. No limits.

u	U	*Comp. Time*	*Comp. Time/Step*	λ_{max}	*Error (%)*	*Number of* Equations
10^{-3}	10	77.5	1.76	0.04956	2.1	523

Table 5.13: Load margin for system reduction and tangent vector. With limits.

Reduced Jacobian Determinant Partitioning and System Reduction Techniques

Table 5.14 shows system reduction mixed with the reduced Jacobian determinant partitioning technique, without generators limits. As expected, this technique does not provide good results.

Table 5.15 shows the results of this technique when generators limits are considered. Once more, a large error is observed, disqualifying reduced Jacobian determinants as partitioning tools.

u	U	*Comp. Time (s)*	*Comp. Time/Step*	λ_{max}	*Error (%)*	*Number of Equations*
10^{-3}	2	47.8	2.99	0.3241	-12.24	493

Table 5.14: Load margin for system reduction and reduced Jacobian determinant. No limits.

u	U	*Comp. Time (s)*	*Comp. Time/Step*	λ_{max}	*Error (%)*	*Number of Equations*
10^{-3}	2	82.8	1.8	0.0611	+33.52	506

Table 5.15: Load margin for system reduction and reduced Jacobian determinant. With limits.

Chapter 6

Conclusions

6.1 Problem Investigated

Static voltage collapse is analyzed in this work. The motivation of the study has been given by several occurrences of this phenomenom around the world. In the search for a voltage collapse index, several techniques are tested and compared, and network partitioning techniques are proposed for computational burden reduction.

6.2 Contributions

The major contributions encountered in this thesis relate to voltage collapse index and network partitioning techniques determination.

– **Voltage collapse indices**

Voltage collapse indices are compared, and shortcomings not addressed by other investigators are discussed in this thesis. It is shown that the singular values and eigenvalues indices (singular value and eigenvalues decomposition) do not enable one to predict the collapse, because of their sharp variations at the bifurcation. A new voltage security index is proposed based on reduced Jacobian determinants with respect to the system critical bus, which is the bus with the largest entry in the right-zero-eigenvector. In contrast to the sharp variation observed for the previous indices, the reduced determinant provides similar quadratic or quartic behavior with respect to a load increase as the test functions of [51], allowing to predict the bifurcation point if no generators limits are considered. Test functions and reduced Jacobian determinants provide the same results when limits are considered, but the desired quadratic or quartic shape is not obtained in this case. Therefore, these indices do not provide good results under realistic conditions, although the results are better than those obtained by eigenvalues and singular values decomposition under the same assumptions.

– **Network Partitioning Techniques**

Load margin determination by continuation methods is time consuming for large power systems, although the results obtained are accurate. In order to reduce this computational burden, several partitioning and reduction techniques are proposed in this thesis. Right eigenvector, tangent vector and reduced Jacobian determinant partitioning techniques are proposed. For each technique, a rank buses vector is obtained, and network partitioning is calculated according to a specified tolerance k. This value k determines the number

of blocks obtained by the partitioning techniques. The load margin obtained when the partitioned systems are considered as isolated power systems does not provide a good voltage security index. However, when one considers these partitioned systems as the areas where load is to be increased, better results are obtained, depending on the choice of k. It is shown that computational burden may be strongly reduced as the system is partitioned. On the other hand, a several-block partitioning may drive one to wrong results.

System reduction technique is based on the elimination of variables that suffer small changes during the voltage collapse process, according to a tolerance value u. The elimination is carried out every U number of steps. It is shown that the values u and U play a very important role on system reduction.

It is shown that of all partitioning methods proposed, the tangent vector technique is the most efficient and accurate of them.

6.3 Future Work

– **Voltage Collapse Index**

A better index to predict proximity to the collapse point when generators limits are considered must be developed. Furthermore, the results obtained with test functions and reduced Jacobian determinant are reasonable when calculated at the critical bus, but this bus becomes critical only when close to the bifurcation, and it cannot be detected for an operating point far from this point. Thus, critical bus determination for an operating point other than saddle-node bifurcation must be studied further.

– **Network Partitioning Techniques**

The partition techniques proposed in this thesis depend on the choice of tolerance k. Determination of this value is an open question, and has crucial importance in the partitioning results.

The system reduction technique depends on the determination of values u and U. In this thesis several values of u and U are tested, but a technique to obtain these optimal values is not provided, and should be studied further.

If system reduction is mixed with tangent vector technique, promising results are obtained. In this case, the values of k, u and U must be determined.

Appendix A

PFLOW Program

This appendix briefly describes the PFLOW program, the C code implementation of direct and continuation methods used in this thesis. The help file provided by the program is shown below, showing the program's options.

```
AC/DC Power Flow (c)1994 C. Canizares and F. Alvarado

Usage:
       Like any other UNIX program, i.e., command-line options (-option)
       with redirection of input (<) and output (>) from screen into files:

              pflow  [-option]  [>]input_file   [>]output_file

Input file:
       The input_file could be in WSCC format (or Anarede's variation) or IEEE
       common format (or Electrocon's variation) for the ac system.  The dc
       data must be in multiterminal ETMSP format, although it just deals with
```

```
       the standard two-terminal HVDC problem.

Output files:
       The program writes the solution into the output_file in ASCII.  It
       can also write the solved case in a file in IEEE common format
       (the HVDC links are written in ETMSP format) using the -W or -w option.
       Additional files can be created for post-processing analyses (see
       options below), such as the bifurcation diagram (nose curve) in column
       form for plotting with MATLAB or other programs, Jacobians for SMMS or
       MATLAB studies, etc.

Solution Technique:
       The ac/dc power flows are solved with simultaneous N-R, allowing for
       asynchronous systems, area interchange, remote voltage control, and
       local and remote regulating transformers (LTCs and phase shifters
       controlling voltages, angles, and/or active and reactive power flows).

Options:
         -a     Turns off tap and angle limits in regulating transformers.

         -A     Turns off interchange area control.

         -b     Solve base case before changing the loading factor lambda.

         -Bnum  PQ bus number 'num' where the voltage is fixed in order to
                find the loading factor (lambda) for voltage collapse studies.
                Must be used with -K and -v options.

         -cfile Increases the loading factor lambda using a continuation
                method for finding voltage profiles.
                The output (optional 'file') is a list of 8 ac voltages that
                change the most, plus 3 additional variables for each dc bus
```

```
       (see -e option).  Must be used with the -K option.

-Cfile Point of Collapse studies, i.e., find the max. loading factor
       lambda for a given generation and load direction. The base case
       loading can be initialized using the -L option; however, the
       program calculates an initial loading of the system before the
       PoC method is applied.  The left e-vector is written in 'file'
       (optional).  Must be used with the -K option.

-d     Generates some debug output.

-Dfile Read load model data from 'file', using Ontario Hydro (OH)
       format, which is based on the load model: Pl=Pn*V^a+Pz*V^2
                                                 Ql=Qn*V^b+Qz*V^2
       If a bus is not defined in the list, Pn=Qn=0 is assumed.

-e     Output dc variables in continuation method.

-Efile Print in 'file' the continuation method direction vector at the
       maximum loading factor (PoC right e-vector).

-f     Output Sensitivity Factors (SF) and Voltage Sensitivity Factors
       (VSF) during non-parameterized continuation method computations.

-Fval  Stability/sparsity value 'val' for factorization (def. 0.01).
       A value of 0 means choose a pivot based on sparsity only;
       a value of 1 means choose a pivot based on stability only.

-g     Force Q in generators to zero when reading data in IEEE
       common format, since sometimes a value of Qg creates
       convergence problems.
```

```
-G      Do not enforce Q limits during the iteration process.  The
        limits will be applied after a base solution has been found.

-h      Prints this message in standard output.

-Hfile Increases the loading factor lambda using a parameterized
        continuation method for finding voltage profiles.
        The output (optional 'file') is a list of 8 ac voltages that
        change the most, plus 3 additional variables for each dc bus
        (see -e option). Must be used with the -K option.

-ifile List of bus numbers and names in 'file' for printing voltage
        profiles with the -c and -H options. The input format is:
        BusNumber BusName; use zero when either the number or the name
        are unknown. If BusName has spaces, wrap it in double or single
        quotes.

-I      Input data in IEEE common format.

-jfile Write the Jacobian of the solved case in I J VALUE format in
        'file.jac'.  The equation mismatches and the system variables
        are also written in 'file.mis' and 'file.var', respectively.
        If no 'file' is given the program writes to standard output.

-Jfile With the -B option, it generates the Jacobian, mismatches
        and variables corresponding to the system without the loading
        factor as a variable.  For PoC studies (-C option) it
        generates the nxn ac/dc system Jacobian, mismatches and
        variables; for the complete (2n+1)x(2n+1) PoC Jacobian, use
        the -j option.

-kval  Factor 'val' used in the homotopy continuation method for
```

```
       finding the increments in the loading factor lambda (def. 1).
       Must be used with the -c and -H options.

-Kfile Read generation and load distribution factors from 'file'.
       All data is assumed p.u. and must be separated by spaces, i.e.,
       BusNumber BusName DPg Pnl Qnl PgMax [Pzl] [Qzl].  If the input
       variables DPg, Pnl, Qnl or PgMax  are unknown, give them a value
       of zero.  Pzl and Qzl are optional.  PgMax is not needed when
       using the -X option; in this case the input data in 'file' is:
       BusNumber BusName DPg Pnl Qnl [Pzl] [Qzl].
       The generation factors are normalized for each area, i.e.,
       ||DPg||=1 per area.
       The load is represented by:
            Pl=(Pn+Pnl*lambda)*V^a+(Pz+Pzl*lambda)*V^2
            Ql=(Qn+Qnl*lambda)*V^b+(Qz+Qzl*lambda)*V^2
       where Pn, Qn, Pz, Qz, a, and b are defined with the -D option,
       and lambda corresponds to the loading factor.  If the -D option
       is not used, the load model default values are: a=b=0, Pz=Qz=0.
       Buses not in the list are assumed to have zero distribution
       factors.   If BusName has spaces, wrap it in double or single
       quotes.

-lfile Write standard error output to 'file' (log file).

-Lval  Loading factor 'val' (def. 0).  Simulates load changes in
       conjunction with the load distribution factors (-K option).

-mnum  Output information to calculate the ac/dc TEF profile for
       voltage collapse studies using MATLAB, with 'num' number
       of significant digits (def. & min. 6, max. 10). '

-Mnum  Number 'num' of max. N-R iterations, overriding input data
```

```
       (default 50).

-n     Turns off all ac system limits.

-N     Turns off all ac system controls.

-otol  The tolerance 'tol' controls the application of limits during
       the continuation process.  The smaller this value, the more
       steps required of the continuation method (default 0.0001).

-O     This option is used together with -m to define the PI
       controller gains (Kp and Ki) of HVDC converters for dc TEF
       computations.  If this option is present, the program reads
       these gains from the console, otherwise it defaults to
       'typical' values of Ki=75 and Kp=1 for all converters.

-p     Turns off P and Q limits in regulating transformers.

-P     Turns off P and Q control by regulating transformers.

-q     Turns off Q limits in PV buses.

-Q     Turns off remote voltage generator control.  The generators
       will just control their terminal voltage to its initial value.

-r     Turns off V limits in regulating transformers and PV buses.

-R     Turns off V control by regulating transformers.

-s     Suppress ASCII output_file.

-Sval  Stop value 'val' for the loading factor lambda in the continua-
```

```
        tion method (-c and -H options), in p.u. of the maximum lambda.
        The default is 0 for a complete trace of the bifurcation
        diagram (min. 0; max. 1, i.e., lambda maximum).

-ttol   If the relative error of two consecutive iteration mismatches
        is larger than 'tol', voltage limits and regulating transformer
        limits are applied (default 0.1).

-Ttol   P.U. tolerance 'tol' for N-R method (default 1e-4).

-uval   Value 'val' of the tolerance used to reduce the number of equa-
        tions in the continuation method (-c and -H options), based on
        the tangent vector technique.
        The default is 1e-3 or 0.1(min. 0 or no reduction, max. 20).
        WARNING: This option might produce cycling, back-tracking, or
                 singularity problems. If this happens, increase the
                 number of steps in the -U option and/or reduce the
                 value of 'val' in -u.

-Unum   Number 'num' of steps of the continuation method (-c and -H
        options) between system reductions.  Used with the -u option.
        The default number is 10 (min. 2, max. 100).

-vmag   Voltage magnitude 'mag' at the first PQ bus (unless otherwise
        specified by -B option) to find the corresponding lambda
        for voltage collapse studies.  Must be used with -K option.

-Vfile Read initial guesses for ac and dc variables from 'file'.
        The data must be separated by spaces, i.e.,
        BusNumber BusName V_mag V_ang(deg), for ac buses, and
        BusNumber BusName Variables Values, for dc buses.
        For defining the dc variable, use the same EPRI format used
```

```
       to define the control modes in the dc lines (e.g., ALGAPA,
       would represent the dc variables Alpha, Gamma and Power);
       the values must be given in standard units, i.e., MW, MVAR, KV,
       Amp, deg.  If the input variables are unknown give them a value
       of zero.  Buses not in the list are given a flat start.  If
       BusName has spaces, wrap it in double or single quotes.

-wfile Write solved case into 'file' in IEEE CARD common format.
       If no 'file' is given the program writes to standard output.

-Wfile Similar to -w option, but the solved case is written in IEEE
       TAPE common format.

-x     Ignore distribution factors for generations during the initial
       power flow solution (use only one slack bus).

-X     Do not enforce maximum active generation limits (PgMax).
       See -K option.

-yfile Print in 'file' an approximation of the left e-vector of the
       smallest real |e-value| at the current operating point.

-Yfile Print in 'file' an approximation of the right e-vector of the
       smallest real |e-value| at the current operating point.
```

Bibliography

[1] G. Brownell and H. Clark, "Analysis and solutions for bulk system voltage instability," *IEEE Computer Applications in Power Systems*, July 1989, pp. 31–35.

[2] IEEE Work Group on Voltage Stability, System Dynamic Performance Subcommittee, "Voltage stability of power systems," technical report 90TH0358-2-PWR, IEEE, 1990.

[3] R. B. Prada, B. J. Cory, and R. Navarro Perez, "Assessment of steady state voltage collapse," *Proc. of the Tenth Power Systems Computation Conference*, Graz, Austria, August 1990, pp. 1189–1195.

[4] CIGRE WG 38.02 Task Force No 10, "Modeling of voltage collapse including dynamic phenomena," technical report of task force 38-02-10, draft 3, CIGRE, June 1992.

[5] V. Ajjarapu, "Identification of steady state voltage stability in power systems," *Proc. of International Conference on High Technology in the Power Industry*, March 1988, pp. 244–247.

[6] F. L. Alvarado and T. H. Jung, "Direct detection of voltage collapse conditions," pp. 5.23–5.38 in [64].

[7] Shui-Nee Chow and Jack K. Hale, *Methods of Bifurcation Theory.* Springer-Verlag, New York Inc., 1982.

[8] I. Dobson, "Observations on the geometry of saddle node bifurcations and voltage collapse in electrical power systems," *IEEE Trans. Circuits and Systems—I*, vol. 39, no. 3, March 1992, pp. 240–243.

[9] I. Dobson and L. Lu, "New methods for computing a closest saddle node bifurcation and worst case load power margin for voltage collapse," IEEE/PES Summer Meeting-Paper 92 SM 587-6 PWRS, 1992.

[10] Y. Tamura, H. Mori, and S. Iwamoto, "Relationship between voltage instability and multiple load-flow power margin for voltage collapse," *IEEE Trans. Power App. and Systems*, Vol PAS-102, no. 5, May 1983, pp. 1115–1125.

[11] H. G. Kwatny, A. K. Pasrija, and L. Y. Bahar, "Loss of steady-state stability and voltage collapse in electric power systems," *Proc. 24th Conference on Decision and Control, Ft. Lauderdale, Fl.*, December 1985, pp. 804–811.

[12] H. G. Kwatny, A. K. Pasrija, and L. Y. Bahar, "Static bifurcations in electric power networks: Loss of steady-state stability and voltage collapse," *IEEE Trans. Circuits and Systems*, vol. 33, no. 10, October 1986, pp. 981–991.

[13] S. Abe et al., "Load flow convergence in the vicinity of a voltage stability limit," *IEEE Trans. Power Apparatus and Systems*, vol. PAS-97, no. 6, November 1978, pp. 183–1985.

[14] EPRI Task Force, "Voltage stability/security assessment and on-line control," technical report TR-101931, EPRI, April 1993. Vol. 1.

[15] G. K. Morrison, B. Gao, and P. Kundur, "Voltage stability analysis using static and dynamic approaches," *IEEE Trans. Power Systems*, vol. 8, no. 3, August 1993, pp. 1159–1171.

[16] P. W. Sauer and M. A. Pai, "Power system steady-state stability and the load-flow jacobian," *IEEE Transactions on Power Systems*, vol. 5, no. 4, November 1990, pp. 1374–1381.

[17] C. A. Cañizares, "Conditions for saddle-node bifurcations in ac/dc power systems," *Electric Power & Energy Systems*, vol. 17, no. 1, 1995, pp. 61–68.

[18] L. Vargas and V. H. Quintana, "Load modeling and eigenvalue computations in voltage stability analysis," *Proc. 0f the 11th PSCC Conference*, Avignon, France, August 1993, pp. 339–343.

[19] C. A. Cañizares, F. L. Alvarado, C. L. DeMarco, I. Dobson, and W. F. Long, "Point of collapse methods applied to ac/dc power systems," *IEEE Trans. Power Systems*, vol. 7, no. 2, May 1992, pp. 673–683.

[20] N. Martins and L. T. G. Lima, "Eigenvalue and frequency domain analysis of small-signal electromechanical stability problems," *Proc. III SEPOPE*, Belo Horizonte, Brazil, paper IP-18, May 1992.

[21] N. Martins, "Efficient eigenvalue and frequency response methods applied to power systems small-signal stability studies," *IEEE Trans. Power Systems*, vol. 73, no. 1, February 1986, pp. 217–226.

[22] P. P. Varaiya, F. F. Wu, and R. L. Chen, "Direct methods for transient stability analysis of power systems: Recent results," *IEEE Transactions*, vol. 73, no. 12, December 1985, pp. 1703–1715.

[23] A. A. Fouad et al., "Direct transient stability analysis using energy functions - application to large power networks," *IEEE Trans. Power Systems*, vol. 2, no. 1, February 1987, pp. 37–44.

[24] T. Overbye, *Application of an Energy Based Security Method to Voltage Instability in Electrical Power Systems*, PhD thesis, University of Wisconsin–Madison, 1991.

[25] C. A. Cañizares, *Voltage Collapse and Transient Energy Function Analyses of AC/DC Systems*, PhD thesis, University of Wisconsin–Madison, 1991.

[26] T. J. Overbye and C. L. DeMarco, "Voltage security enhancement using energy based sensitivities," *IEEE Trans. Power Systems*, vol. 6, no. 3, August 1991, pp. 1196–1202.

[27] C. L. DeMarco and C. A. Cañizares, "A vector energy function approach for security analysis of ac/dc systems," *IEEE Trans. Power Systems*, vol. 7, no. 3, August 1992, pp. 1001–1011.

[28] T. Juan et al., "Emergency Load Shedding to Avoid Risks of Voltage Instability Using Indicators," IEEE/PES Winter Meeting - Paper 93 WM 097-6 PWRS, Atlanta, GA, February 1993.

[29] T. Van Cutsem, "A method to compute reactive power margins with respect to voltage collapse," IEEE/PES 90 WM 097-6 PWRS, February 1990.

[30] H. J. C. P. Pinto et al., "Modal analysis for voltage stability: Application at base case and point of collapse," in [65].

[31] Julián Barquin and T. Gómez, "Determination of voltage collapse areas through generalized singular value analysis," in [65].

[32] A. C. Z. de Souza and V. H. Quintana, "Identification of voltage collapse using network partitioning," *Proc. NAPS*, October 1993, pp. 191–196.

[33] A. C. Z. de Souza and V. H. Quintana, "Identification of voltage collapse margins in power systems," *CCECE/CCGEI Proceedings*, September 1993, pp. 933–937.

[34] A. C. Z. de Souza and V. H. Quintana, "A new technique of network partitioning for voltage collapse margin calculations," *IEE Proc.-Gener. Transm. Distrib.*, vol. 141, November 1994, pp. 630–636.

[35] Yakout Mansour, "Industry practice in voltage stability analysis of power systems," in [65].

[36] C. A. Cañizares, A. Z. de Sousa, and V. H. Quintana, "Improving continuation methods for tracing bifurcation diagrams in power systems," in [65].

[37] L. Vargas and V. H. Quintana, "Clustering techniques for voltage collapse detection," *Electric Power System Research*, vol. 23, no. 1, 1993, pp. 53–59.

[38] B. Gao, G. K. Morrison, and P. Kundur, "Voltage stability evaluation using modal analysis," *IEEE Trans. Power Systems*, vol. 7, no. 4, November 1992, pp. 1529–1542.

[39] R. A. Schlueter, I. Hu, and M. W. Chang, "Methods for determining proximity to voltage collapse," IEEE/PES Winter Meeting - Paper 90 WM 096-8 PWRS, 1990.

[40] M. M. Begovic and A. G. Phadke, "Voltage stability assessment through measurement of a reduced state vector," *IEEE Trans. Power Systems*, vol. 5, no. 1, February 1990, pp. 198–203.

[41] M. A. Pai, *Stability of Power Systems by Lyapunov's Direct Method*, volume 3. North-Holland Systems and Control Series, 1981.

[42] D. J. Hill, "Nonlinear dynamic load models with recovery for voltage stability studies," *IEEE Trans. Power Systems*, vol. 8, no. 1, February 1993, pp. 166–176.

[43] P. A. Löf, T. Smed, G. Anderson, and D.J. Hill, "Fast calculation of a voltage stability index," *IEEE Trans. Power Systems*, vol. 7, no. 1, February 1992, pp. 54–64.

[44] W. W. Price et al., "Load representation for dynamic performance analysis," IEEE/PES Winter Meeting-Paper 92 WM 126-3 PWRD, January 1992.

[45] C. A. Cañizares, "On bifurcations, voltage collapse and load modeling," IEEE/PES 94 SM 512-4 PWRS, San Francisco, CA, jul 1994.

[46] P. A. Löf, T. Smed, G. Anderson, and D.J. Hill, "Voltage dependent reactive power limits for voltage stability studies," IEEE/PES Winter Meeting-Paper 94 WM 248-5 PWRS, jan 30 - feb 3 1994.

[47] C. A. Cañizares and S. Hranilovic, "Transcritical and Hopf bifurcations in ac/dc systems," in [65].

[48] Julián Barquin, Tomás Gómez, and F. Luis Pagola, "Estimating the loading limit margin taking into account voltage collapse areas," IEEE/PES Winter Meeting-Paper 95 WM 183-4 PWRS, jan 29 - feb 2 1995.

[49] P. Marannino, P. Bresesti, M. Delfanti, G. P. Granelli, and M. Montagna, "Voltage collapse proximity indicators for very short term security assessment," in [65].

[50] C. A. Cañizares, A. C. Z. de Souza, and V. H. Quintana, "Comparison of performance indices for detection of proximity to voltage collapse," IEEE/PES Summer Meeting-Paper SM PWRS, 1995.

[51] H-D Chiang and R. Jean-Jumeau, "Toward a practical performance index for predicting voltage collapse in electric power systems," IEEE/PES Summer Meeting-Paper 93 SM 512-4 PWRS, July 1994.

[52] I. Dobson and H. D. Chiang, "Towards a theory of voltage collapse in electric power systems," *Systems & Control Letters*, vol. 13, 1989, pp. 253–262.

[53] C. A. Cañizares and F. L. Alvarado, "Point of collapse and continuation methods for large ac/dc systems," *IEEE Trans. Power Systems*, vol. 8, no. 1, February 1993, pp. 1–8.

[54] R. Seydel, *From Equilibrium to Chaos–Practical Bifurcation and Stability Analysis*. Elsevier Science, North-Holland, 1988.

[55] Ferdinand Verhulst, *Nonlinear Differential Equations and Dynamical Systems*. Springer-Verlag, 1989.

[56] H. D. Chiang and F. F. Wu, "Stability of nonlinear systems described by a second-order vector differential equations," *IEEE Trans. Circuits and Systems*, no. 6, June 1988, pp. 703–711.

[57] A. M. Erisman I. S. Duff and J. K. Reid, *Direct Methods for Sparse Matrices*. Oxford Science Publications, 1986.

[58] G. Gollub and C. F. Van Loan, *Matrix Computations*. Johns Hopkins, London, fourth edition, 1993.

[59] Ben Noble and J. W. Daniel, *Applied Linear Algebra.* Prentice-Hall, New York, third edition, 1988.

[60] E. R. Barnes, "An algorithm for partitioning the nodes of a graph," *SIAM Journal on Algebraic and Discrete Methods*, vol. 3, no. 4, 1982, pp. 541–550.

[61] Scott W. Hadley, Brian L. Mark, and Anthony Vannelli, "An efficient eigenvector approach for finding netlist partition," *IEEE Transaction on CAD/ICAS*, vol. 11, no. 7, July 1992, pp. 885–892.

[62] C. M. Fidduccia and R. M. Matheyses, "A linear-time heuristic for improving network partitions," *Proc. 19th Design Automation Workshop*, 1982, pp. 175–181.

[63] The Math Works Inc., Natick, Massachusetts, *MATLAB*, 1993.

[64] L. H. Fink, editor, *Proc. Bulk Power System Voltage Phenomena—Voltage Stability and Security*, EL-6183, EPRI, January 1989.

[65] L. H. Fink, editor, *Proc. Bulk Power System Voltage Phenomena III—Voltage Stability and Security*, ECC Inc., Fairfax, VA, August 1994.